THE FLORIDA STATE UNIVERSITY

COLLEGE OF ARTS AND SCIENCES

VARIABILITY OF FIVE DAY WIND FIELDS

OVER THE INDIAN OCEAN

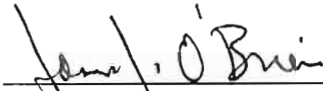USING SHIP AND SASS DATA

By

KELLEY FRANKLIN MILES

A Thesis Submitted to the
Department of Meteorology in partial
fulfillment of the requirements for
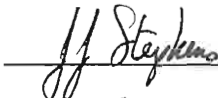the degree of Master of Science

Degree Awarded:

Fall Semester, 1992

Fall Semester, 1992

The members of the Committee approve the thesis of Kelley Franklin Miles, defended on November 6,1992.

James J. O'Brien
Professor Directing Thesis

J. J. Stephens
Committee Member

Kevin A. Kloesel
Committee Member

Approved:

David W. Stuart, Chair, Department of Meteorology

David W. Stuart, Chair, Department of Meteorology

Acknowledgements

I would like to thank Dr. J.J. Stephens and Dr. Kevin Kloesel for their willingness to serve on my committee. Their input and interest in my research is much appreciated.

I would like to thank all of the members of MASIG for their support and friendship during my graduate work at Florida State. Special thanks goes to Dr. David Legler for his tireless work in backing my research with his time and invaluable comments. Thanks to Dr. Steve Meyers for helping me labor through the mathematics and to Al Davis and James Stricherz for answering my many computer questions. Rita Kuyper and Patty Boutelle also deserve recognition for their efforts in keeping me organized and moving in the right direction. I also must thank Cathy Stephens Jones, my fellow thesis writer, without whose collaboration I would have never been able to finish.

I wish to express sincere gratitude to Dr. James O'Brien for his many hours of advice, encouragement, and teaching. He provided me with a great opportunity for learning and advancing in many areas of education which I can only hope someday to repay.

My greatest thanks goes to my Heavenly Father through whom all things are possible. Through Him, I have received suppport from my wife, Christine. I wish to thank her for the encouragement, support, late nights, hot meals, and unconditional love that she never failed to give.

Table of Contents

List of Tables

List of Figures

Abstract

A variational method is adapted to produce five-day averaged wind fields from SEASAT scatterometer and ship data with one-degree resolution for the 1978 summer monsoon period over the Indian Ocean. A cost functional, containing five terms, measures the closeness of the resultant field to input data, the smoothness of the data compared to climatological values, and approximations to the kinematic properties of divergence and curl of the climatology.

The variational method is used first for 30-day results over the Indian Ocean. Ten and five-day results are then calculated, each based on the previously determined longer term results. The results reveal five-day time scale information about the intramonsoonal variability of the region in six areas of interest including the monsoon and trade wind regions. The position of the Findlater Jet is found to be southwest of the mean position and the trade winds appear to be stronger than normal throughout this monsoon period.

A sensitivity analysis is performed on the results to determine the effects of the free parameters of the variational scheme on different response functions. This objective method determines the free parameters of the cost functional terms. The wind magnitudes are found to be most sensitive to the smoothing term especially in regions of erroneous or noisy data. The functional terms. The wind magnitudes are found to be most sensitive to the smoothing term especially in regions of erroneous or noisy data. The smoothing term is also the only one to have a negative effect on the

response function, i.e. the only term which when increased (decreased) results in a decrease (increase) in the overall wind magnitudes. The curl of the winds were found to be most sensitive to the scatterometer data term especially in regions of sparse ship data. Here two of the four parameters have negative effects on the overall curl and therefore decrease the average curl of the field with increasing weight value.

1. Introduction

Estimating wind fields over the northern hemisphere oceans on monthly time scales is possible with conventional ship data. The southern hemisphere has comparatively little ship or buoy data. Creating wind fields on weekly time scales from these data is necessary to retain important synoptic scale information. Unfortunately, many of the available observations contain instrument, measurement, and transmission errors (Pierson 1990; Legler *et al.* 1989; Legler 1992). In order to use the vital information contained in the observations but remove erroneous data, this study uses a variational technique originally developed by Sasaki in the 1950's and developed by Stephens in the 1960's in which models of the atmosphere are developed (see Sasaki 1958 and Stephens 1965). These models are improved upon in the 1980's by Hoffman (1982, 1984) by introducing additional constraints into the minimization of a cost functional. The direct minimization technique in this study is an attempt to improve the technique applied by Legler *et al.* 1989 to combine in situ data with satellite data to obtain 30-day wind fields over the Indian Ocean. Ten and five-day mean fields are also computed and the short term variability of the study region is examined. These five-day wind fields are important not only to examine the monsoon region and Indian rainfall, but also to study the study region is examined. These five-day wind fields are important not only to examine the monsoon region and Indian rainfall, but also to study the heat budget over the ocean and apply the information to ocean models

(Bruce (1983)). In addition, the effectiveness of remotely sensed data can be evaluated as the observations are used to supplement the conventional ship data. These wind field analyses are also useful in many commercial application areas, such as offshore drilling rigs, the fishing industry, ocean mining, and ship routing (O'Brien *et al.* (1982)).

Many techniques have been used to deal with the problem of the lack of available data over the open ocean. Rao *et al.* (1978) used air trajectories to calculate wind fields over the equatorial Indian Ocean. Estoque and Fernandez-Partagas (1980) were able to study a very small area of the monsoon synoptic wind fields by blending conventional data with satellite observations. The study did not use a minimization scheme or any type of climatology to enhance the wind fields. Utilizing the available satellite observations, Stout and Young (1983) calculated the geopotential field by using satellite wind fields over the Indian Ocean. Harlan and O'Brien (1986) assimilated scatterometer wind fields into surface pressure fields over the North Atlantic to examine the 1978 *QE II* storm.

Based on the effectiveness of the combination of ship and Sea Satellite-A microwave scatterometer (SASS) data given by Estoque and Fernandez-Partagas (1980), Harlan and O'Brien (1986), and Legler *et al.* (1989) for example, this study will use SASS data to improve five-day wind fields of conventional data over the Indian Ocean. The reasons for this combination are that the coverage of the ship data is concentrated near land and in narrow shipping lanes and the coverage of SASS data is more complete. Since the monsoon region is one of the most variable regions in the world narrow shipping lanes and the coverage of SASS data is more complete. Since the monsoon region is one of the most variable regions in the world on the synoptic scale, a study of the five-day variability will yield specific information unavailable from climatologies or scattered ship observations.

This study will prove more efficient in determining a one-degree gridded analysis on the five-day time scale because it includes the reliability of the ship data, the good coverage of the SASS data, and some knowledge of climatological data. In addition to its effectiveness, this study is different from other direct minimization studies due to its use of satellite observations and its short time scale analysis of such a large study region.

It will be found that the combination of ship and SASS data as well as climatological constraints creates a realistic and viable wind field on five-day time scales. In areas of sparse ship data where perhaps one observation is made during a five, ten, or even 30-day period, the data are unrepresentative of the true synoptic scale features. These regions present problems due to the diminished certainty in the data. The 30-day results contain intramonsoonal variability that is evident throughout the ten and five-day results. The validity of this variability and the ability of the minimization technique to represent it is the focus of the study.

A sensitivity analysis performed on the 30-day results contains information on the ability of the constraints in the functional to affect the results. This analysis calculates parameters which show how the weights and associated constraints in the functional affect the results. Global and local sensitivity parameters will show and quantify that the different constraints have different effects overall and in specific areas of the study region. These parameters reveal areas of high or low sensitivity of each of the constraints in the cost functional. As these weights are varied, the influence of the constraints varies and ultimately changes the resultant the constraints in the cost functional. As these weights are varied, the influence of the constraints varies and ultimately changes the resultant fields. The weights are estimated based on criteria that measure these changes in the resultant field. These critieria are based upon what can be

determined to be the true solution based on well sampled areas. These weights are then deemed the "best," or optimal, weights for the study. Finally, an rms-type error, the local sensitivity error, will be calculated to show how small errors in the results occur as a function of uncertainty in the weights, thus allowing for a margin of error in the selection of the optimal weights.

The study begins with a description of the data that will be used in the objective analysis in section 2. Section 3 explains the variational objective analysis method. Section 4 describes the results and their variability. A sensitivity study of the results will be discussed in section 5 and a summary and conclusions will be given in section 6.

2. Data Sets

2.1 COADS CMR5 Ship Data

The ship wind reports for this study are obtained from CMR5 Comprehensive Ocean Atmosphere Data Set (COADS) (Slutz, *et al.* (1985)). The data are extracted from COADS for the Indian Ocean region, 25°E to 125°E, 32°S to 32°N. Data from the time period 7 July 1978 to 10 October 1978 coincide with the Sea Satellite (SEASAT) mission. Ship observations for all five, ten and 30-day periods in the SASS data set are averaged into 1° by 1° boxes. For each of these periods throughout the study period, observations of wind speed greater than three standard deviations from the mean of the domain for that period are considered to be in error and taken out of the data set. Less than one percent of the observations are eliminated by the criterion.

2.2 SASS Data

Originally, the ERS-1 scatterometer data were selected to be used in the minimization technique. Unfortunately, due to serious problems with the initial data from this satellite, the data are not useful in research. In the future, these data could be used to study more recent events in the monsoon and other regions. Instead, much older, but more reliable data information future, these data could be used to study more recent events in the monsoon and other regions. Instead, much older, but more reliable data information will be used. Data from the SEASAT-A microwave scatterometer (SASS)

will be used for the period 7 July 1978 to 10 October 1978. The surface wind direction and speed are determined from scatterometer measurements of backscattered radar signals. The strength of the signal varies with the roughness of the surface and therefore the strength of the wind. The individual data are accurate to $\pm$ 2 m s^{-1} and $\pm$ 20° in direction. SASS estimates wind vectors at a height of 19.5 m over the open ocean on a 100 km grid with dual swaths on either side of the satellite path. The original SASS vectors had problems due to biases and aliases either with the instrument itself or with the model parameterization of the winds (Wentz (1986)). Before dealiasing, the SASS vectors were actually as many as four different wind vector solutions, or aliases, for each observation location. Each of these vectors had approximately the same magnitude, but different directions. The data used in this study are the dealiased SASS data from Wentz (1986) with aliases chosen according to Kalnay and Atlas (1986). Because of the dealiasing scheme, no dealiased solutions are available within 2° - 4° of land. The data coverage is much more evenly spaced than conventional ship data and coverage on time scales of a few days is nearly complete (Figure 1). All available SASS data will be used as a supplement to the ship data in this study.

2.3   FSU Climatological Winds

The FSU climatological winds (see Legler *et al.* 1989; Legler 1991a) for July through October over the Indian Ocean were stored on a one-degree The FSU climatological winds (see Legler *et al.* 1989; Legler 1991a) for July through October over the Indian Ocean were stored on a one-degree grid for the study region. The data were converted from the stored

pseudostress components, τ_x and τ_y, into the u and v components of the wind using the formulae,

$$V = \left(\tau_x^2 + \tau_y^2\right)^{1/4}$$

$$u = \frac{\tau_x}{V} \quad , \quad v = \frac{\tau_y}{V}$$

These winds are nine-year means (1977 - 1985) for each calendar month of the year.

These climatological data represent a unique region of the world where the winds reverse during the course of the year (Hastenrath 1991; Ramage 1971; Yasunari 1991) (Figure 2). The summer monsoon season extends from July to early October before beginning the transition into the winter monsoon with lasts until January. The winds exhibit their largest magnitude in July during the southwest monsoon over the Arabian Sea and the Bay of Bengal. The winds decrease in magnitude near the equator but demonstrate strong, steady southeast trades in the Southern Hemisphere. The South China Sea region also has strong winds that change direction with the monsoon. Through the period of August to October, the Arabian Sea and Bay of Bengal monsoon winds decrease in magnitude slowly and begin to reverse. A strong line of convergence and wind reversal forms in the South China Sea. The steady trade winds in the Southern Hemisphere continue while the winds west of Australia strengthen and are directed toward the north. The smallest magnitude winds occur in the southwestern continue while the winds west of Australia strengthen and are directed toward the north. The smallest magnitude winds occur in the southwestern region of the Indian Ocean.
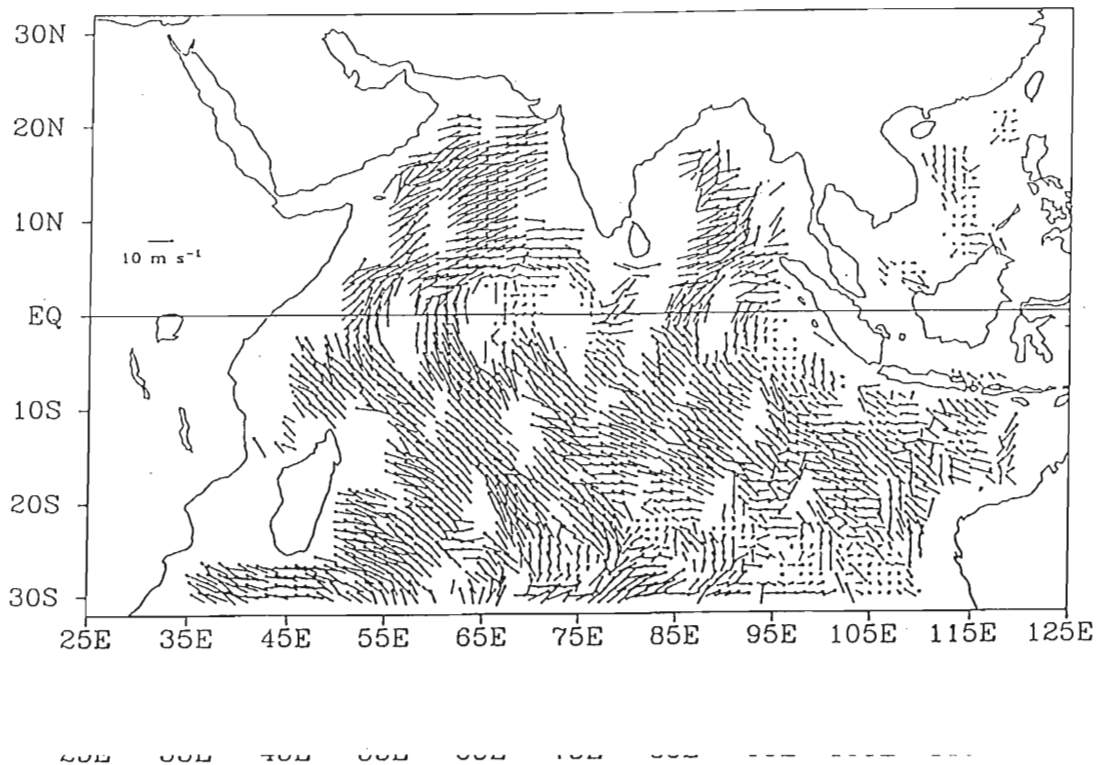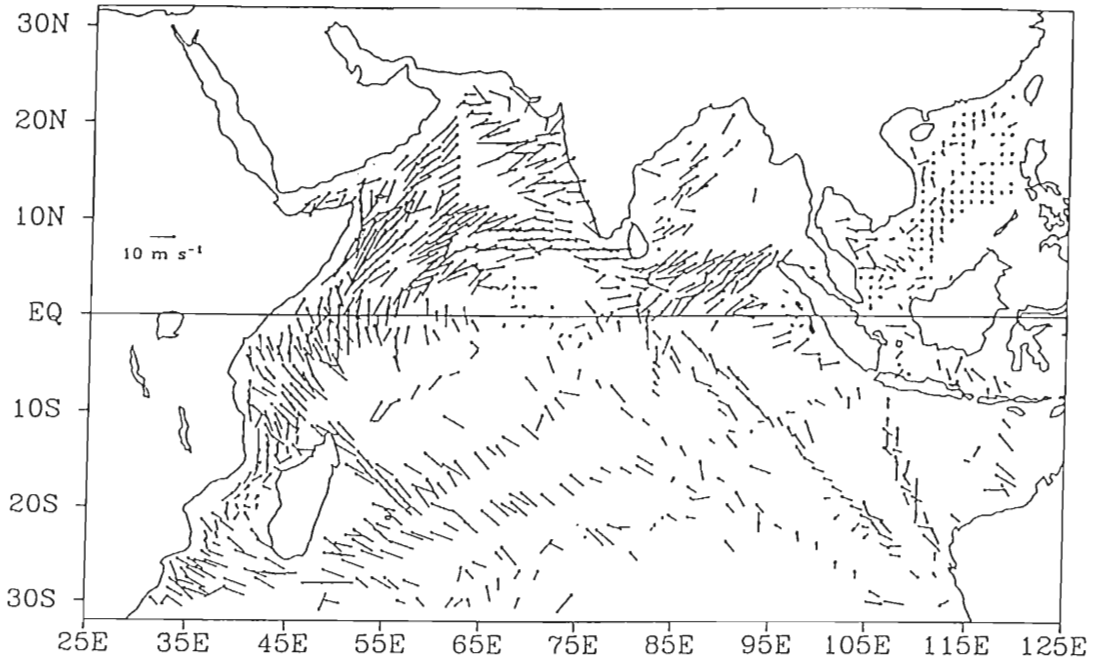
Figure 1.   Typical five day coverage (7 July to 12 July 1978) of ship data (top) and SASS data (bottom) each average on a 1° grid.
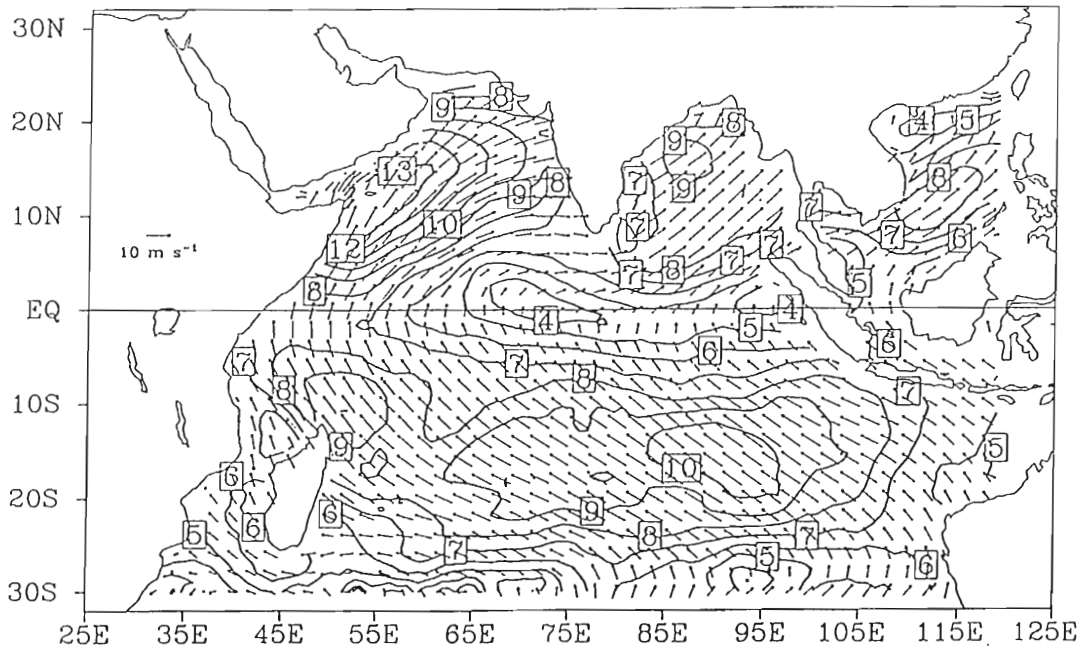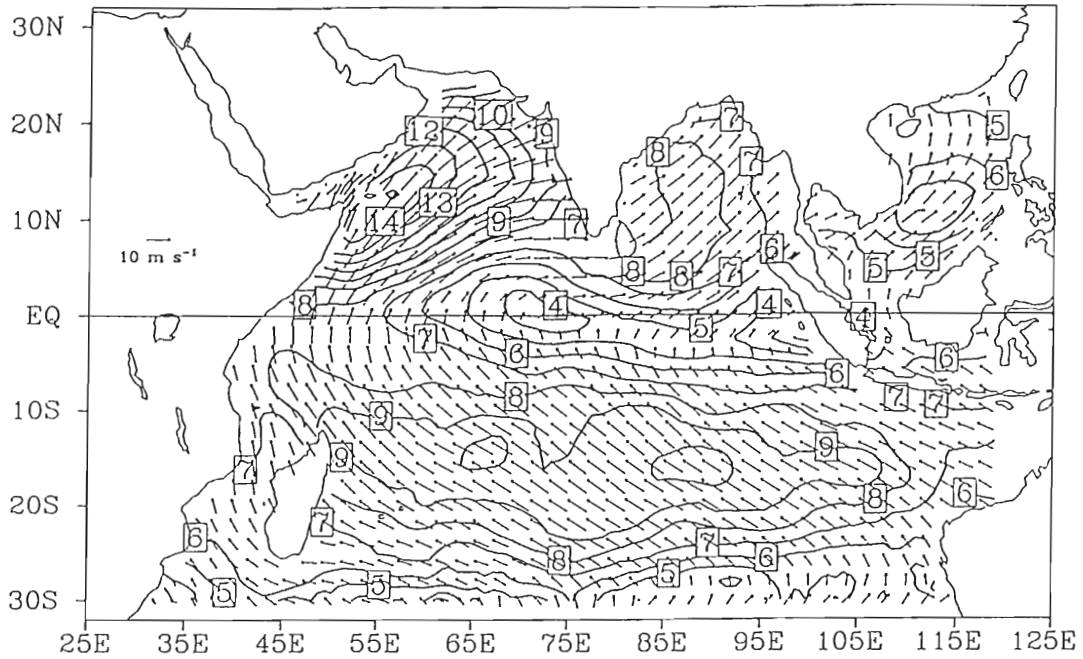
9

Figure 2.   The FSU climatological winds from original pseudostress for
~~the Indian Ocean region for the month of July (top) and August~~

Figure 2.   The FSU climatological winds from original pseudostress for
the Indian Ocean region for the month of July (top) and August
(bottom). Contours are of vector magnitude in m s^{-1}.
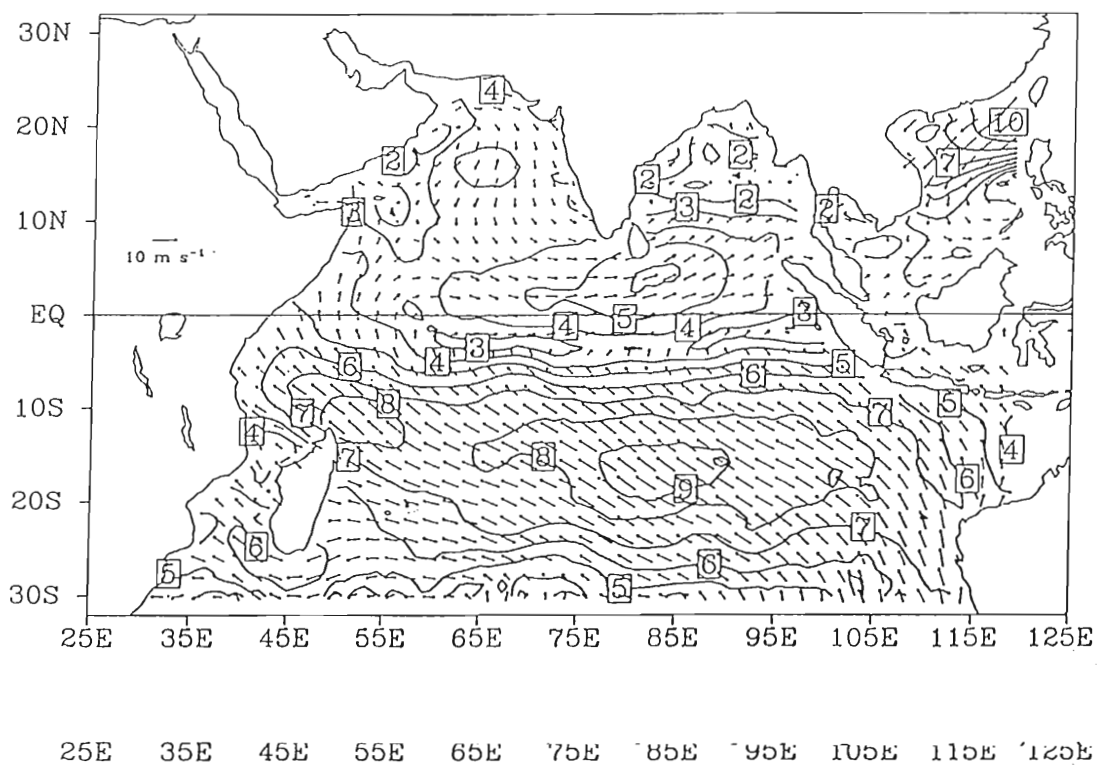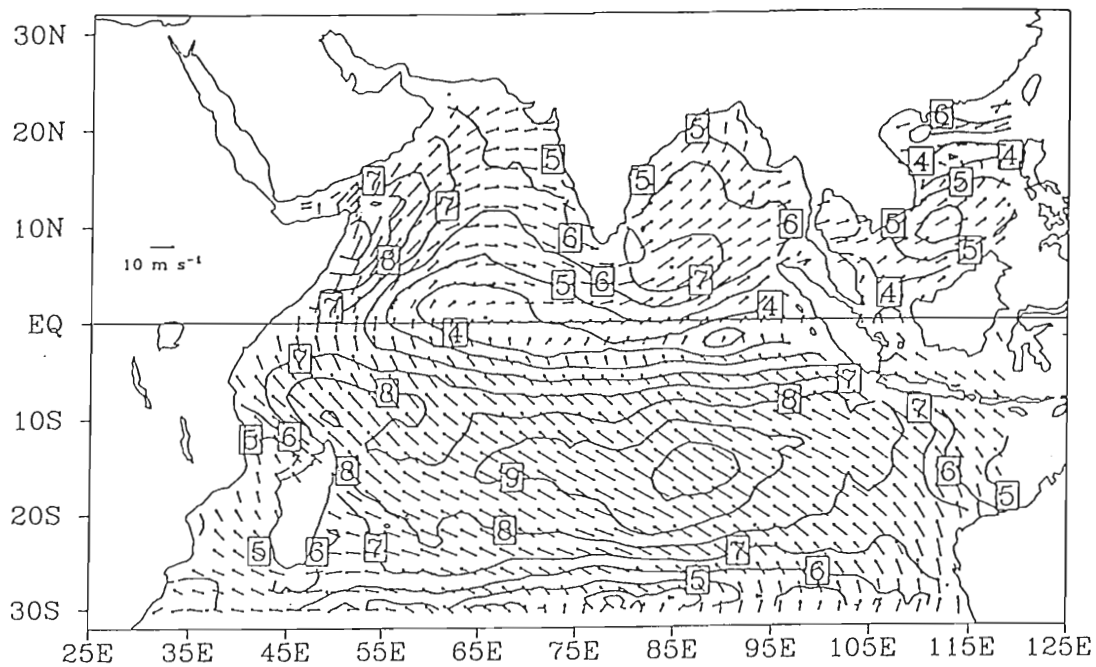
Figure 2.   (Continued)   Climatological winds for September (top) and October (bottom).

3. Data Analysis Method

This study uses a variational scheme called direct minimization, in order to provide gridded wind fields. This objective analysis technique has been used on other data sets and other meteorological parameters (see Sasaki 1958; Stephens 1965; Hoffman 1982, 1984, Legler *et al.* 1989, and Legler 1992). The direct minimization technique defines a positive definite cost functional which is minimized. The individual terms of the functional represent the lack of fit of several factors including kinematic properties of the wind to different aspects of the resulting wind field. Climatological kinematic patterns of divergence and curl are used as constraints in order to help form proper kinematics of the resulting fields. The ship and SASS observations are used in the cost functional to constrain the resulting field to conform to the data. The Laplacian of the climatology also is used to have a smoothing effect on the results by placing a constraint on the Laplacian of the results.

The cost functional used to produce objective wind fields is shown below. The idea is basically a least squares fit to the combination of these data. The solution must be found such that the cost functional, F, is a minimum. That is, the solution and the data are in agreement as closely as possible under the criteria used. We require that the weighted sum of the squares be a minimum and that the weights be reflected by the importance of the constraint that they criteria used. We require that the weighted sum of the squares be a minimum and that the weights be reflected by the importance of the constraint that they multiply in the cost functional.

11

$$F =$$

$$\alpha \sum_{x,y} n_{ship}(x,y)\left[(u - u_{ship})^2 + (v - v_{ship})^2\right]$$

$$+ \quad \beta \sum_{x,y} n_{sass}(x,y)\left[(u - u_{sass})^2 + (v - v_{sass})^2\right]$$

$$+ \quad L^4 \delta \sum_{x,y} \left[(\nabla^2(u - u_{clim}))^2 + (\nabla^2(v - v_{clim}))^2\right]$$

$$+ \quad L^2 \lambda \sum_{x,y} \left(\vec{\nabla} \cdot (\vec{V} - \vec{V}_{clim})\right)^2$$

$$+ \quad L^2 \eta \sum_{x,y} \left(\hat{k} \cdot \vec{\nabla} \times (\vec{V} - \vec{V}_{clim})\right)^2$$

The components of the averaged ship and SASS observations are u_{ship}, v_{ship} and u_{sass}, v_{sass}, respectively. The components of the climatological wind, $\vec{V}_{clim}$, are u_{clim} and v_{clim}.

It is important to have uniform dimensions for each term. Therefore, the last three terms are multiplied by a length scale, L. The value of L is one-degree latitude in order to make all of the terms the same dimension.

The ship and SASS data are weighted by the logarithm of the number of observations that are available in each grid box in order to have a smoother transition of weights between grid boxes with different numbers of observations. Thus, in a box with no observations, the weight is set to zero and in a box with ten observations, the weight is set to one. For the ship data, this is observations. Thus, in a box with no observations, the weight is set to zero and in a box with ten observations, the weight is set to one. For the ship data, this is simply the total number of observations in each period. For the SASS data, the

observations on a given single pass of the satellite in each grid box are summed into a composite observation. It is these composite observations that are totaled and averaged together like the ship observations. The averaged ship and SASS data are used as the initial guess for the minimization so that the resultant field will contain all specific characteristics dictated by the actual observations.

The coefficients, or weights, (α, β, δ, λ, η) allow each term to be weighted according to the determined contribution to the functional. The weights are not defined by the minimization technique and must be determined for each independent study. Since they are all chosen relative to one another, the arbitrary choice of the first weight being set to unity is made. Criteria are used here that give guidelines for the choice of the remaining weights. The four remaining free weights are chosen subjectively based on the terms they multiply. Each term contributes differently to the results and are shown via the criteria discussed in section 4.1 that the weights may be considered as tuning parameters for the results (see also Hoffman (1984)). Careful experimentation using these criteria allow each weight to be determined.

The terms in the functional each represent a different quantity to be minimized. The first term is the data misfit of the resulting wind field to the averaged ship data wind field. The minimum forces the results to agree with the input ship velocity. The ship data also are used as the first guess of the solution and the weight of this term, α, is arbitrarily set to unity. Any initial guess field, i.e. a constant field, should eventually lead to the minimum of the cost functional. However, a better first guess leads to faster convergence of the technique. The second term similarly forces the fit except to the averaged SASS cost functional. However, a better first guess leads to faster convergence of the technique. The second term similarly forces the fit except to the averaged SASS data. The last three terms describe indirect fits to the climatology of the Indian Ocean. The third term is the Laplacian of the difference between the resulting

and climatological winds. This term smoothes the winds and forces connectivity between consecutive locations on the grid. The next term is one of two kinematic constraints. It requires the fit to be similar to the climatological divergence. The last term requires of the curl of the climatological winds to be similar to the results. Hoffman (1984) experimented with the use of these kinematic constraints to determine their usefulness. He found improvements in the wind fields using the new kinematic terms relative to his previous study (Hoffman (1982)). Legler *et al.* (1989) also experimented with these terms and the sensitivity of the results to them. He found that changes in the divergence term had little effect on the curl field and vice versa. The sensitivity analysis in section 5 describes the effects of changes in the weights on different response functions. It is found that small changes in each of the weights results in changes in the resultant field. These changes are measured and incorporated into the selection of the optimal weights. The sensitivity analysis also reveals the importance of each term to the functional by noting these changes.

In order to minimize this functional, the initial values of u and v are varied in order for some minimum to be found. There are several techniques for finding this minimum of the functional (Gill *et al.* (1981) pp. 94-149). Some techniques compute the gradient of the function and determine a search direction, typically down the gradient, and then take as many steps in that direction as necessary to reach the solution. Of the methods described in Gill *et al.* (1981), the conjugate gradient method is the fastest and most efficient. It requires very little computer time or storage and is appropriate for obtaining results for large amounts of data (Navon and Legler 1987; Hoffman 1984). The requires very little computer time or storage and is appropriate for obtaining results for large amounts of data (Navon and Legler 1987; Hoffman 1984). The method works well for this case since the functional is quadratic and has a determinable minimum. A global minimum is not necessarily achieved in the

minimization based on the fact that the Hessian matrix that is calculated is not necessarily positive definite or that the cost functional does not necessarily have positive constant second derivatives. The minimization is not converging to a local minimum because when different initial guesses are used, the solution is very nearly the same. That is, when started in a different location in the gradient field, the solution continues to converge to the same minimum, not several different ones. The iterative scheme stops when the norm of the gradient is reduced by nearly four orders of magnitude. The typical number of iterations in this study is between 15 and 30. The minimization is accomplished using code described in Shanno-Phua (1980).

4. Results

In order to determine the resultant fields, the best possible weights for each of the constraints in the functional must be selected. This is done by first determining the relative impact of each weight, i.e. its effects on the resultant field. The criteria for weight selection are to make sure: the smoothing effects of the functional do not remove local information, the kinematic fields of divergence and curl are realistic, positions of synoptic and monsoon features based on ship means are retained, and the effects of each constraint based on the sensitivity analysis in section 5 are determined.

Upon selection of the weights, minimization of the three 30-day resultant fields are performed. These fields are examined for intramonsoonal variability features and compared to climatology to determine the effects of the minimization. Then, the selected weights are used in the minimization technique for the ten-day resultant fields. The data from these nine ten-day fields are used as the "climatology" for the calculation of the 18 five-day fields. Finally, the variability of these five-day wind fields is carefully examined and noted with emphasis on six specific regions.

4. 1   Weight Selection

The minimization is performed using the 30-day averaged data sets to

obtain results. Initially, all of the weights in the functional are set to unity. The

procedure used for determining the weights is: adjust each of the weights and examine the effects on the resultant field, compare these adjusted resultant fields to well sampled ship data regions by calculating difference fields and correct large biases by further adjustment of the weights, perform a data void test to quantify local effects and errors of the weight changes by removing a region of data and allowing the minimization to replace it with similar wind patterns, and use the sensitivity analysis described in section 5 and knowledge of the system to determine if a small change in the weights is beneficial to the results. Figure 3, described below, shows some of the experiments performed on the results by varying the weights.

The first variable weight β (SASS data), has a large effect on the results, especially in regions where there are few ship observations. Recall also that the ship and SASS data are weighted by the number of observations in a grid box. The SASS data itself is very smooth and contains much less spurious data than the ship observations. It does therefore act as a type of smoothing term for the results. If the weight is too large, the information from the ship observations is lost and the more reliable observations are smoothed out. The SASS data should enhance the ship data and fill in areas where the ship data do not exist. The SASS data should not dominate the results. Its weight β therefore is chosen to be the same as the weight for the ship data.

The second weight, δ, is for the term containing the Laplacian of the results minus climatology. It determines the smoothness of the results. This is an important term in the functional and the results are very sensitive to the weight of this term. The smoothing helps to remove any extremely poor ship an important term in the functional and the results are very sensitive to the weight of this term. The smoothing helps to remove any extremely poor ship data in the field. It becomes crucial to balance this term with the other terms. If the weight is too large, the important high resolution information contained in

18

Figure 3a. (Top) The SASS data for the period 7 July to 6 August 1978. (Bottom) The results for the same period. The weights chosen are

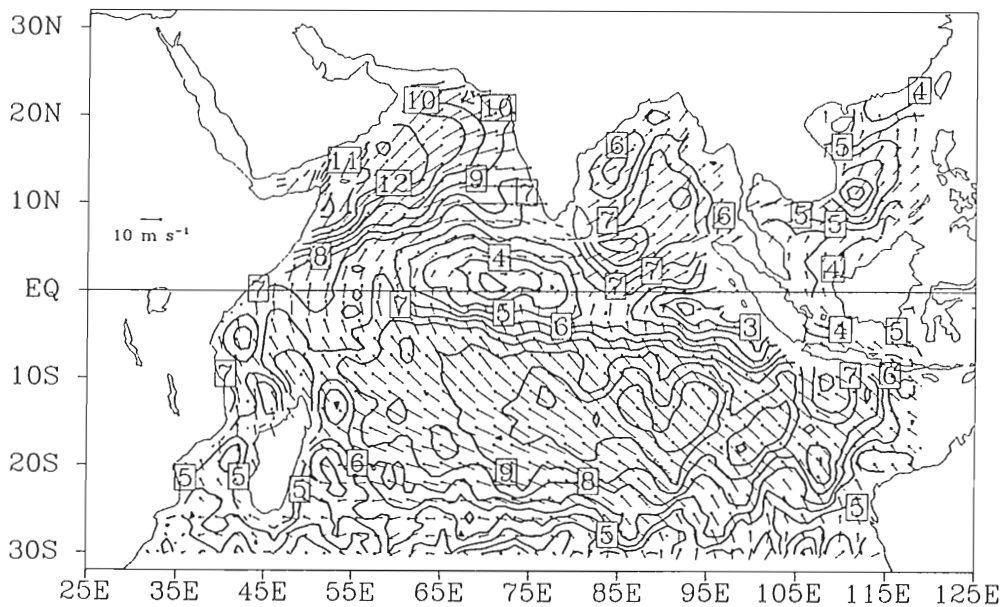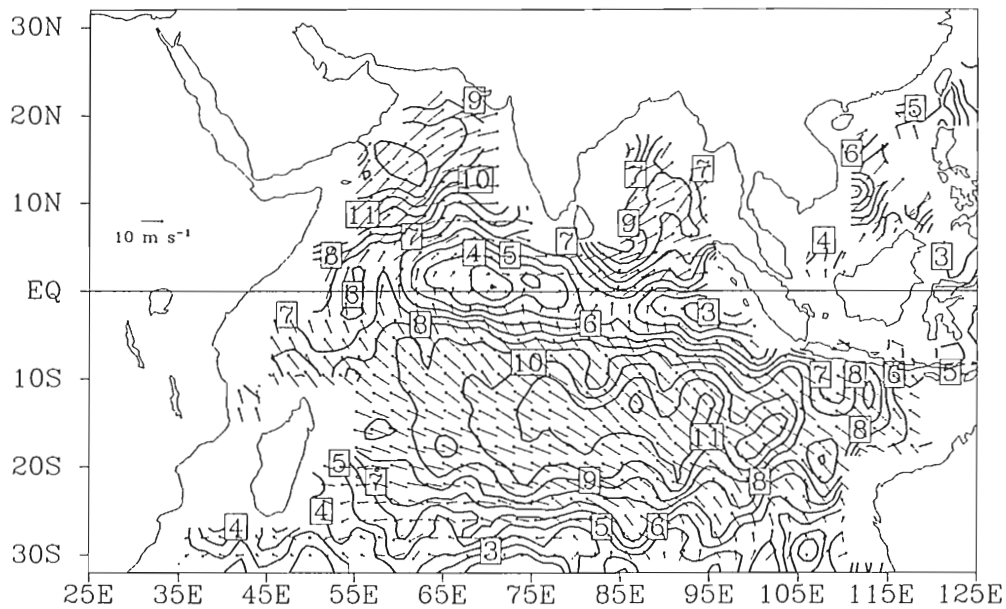Figure 3a. (Top) The SASS data for the period 7 July to 6 August 1978. (Bottom) The results for the same period. The weights chosen are $\beta = 10, \delta = 1, \lambda = 1, \eta = 1$. The figure shows the domination of the SASS data and lack of fit to the climatology in the results. Contours are of vector magnitude (in m s^{-1}).

the ship and SASS data will be smoothed out of the resultant field. If the weight is too small, the results will not exhibit the continuity required for 30-day averaged fields. Figure 3b shows how the smoothing term removes the noise from the first guess field. This experiment is designed to show the effectiveness of the smoothing term. The weight selected for the experiment is much to large to be used in the minimization because it quickly smoothes out the important local information in the results. The region as a whole is smoothed well. However, if this term is set too large, the resultant field begins to resemble climatology and the determination of five-day time scale information becomes impossible. The final selection of this weight also is determined to be the same as the weight for the ship data, i.e. $\delta = 1$.

The first of the two kinematic terms describes the fit to the climatological divergence. The weight for this term is represented by λ. Since the value of this weight should be determined more by its ability to change the divergence field from the initial and climatological fields rather than its ability to change the results, the divergence fields are examined. Since the results are not very sensitive to the term, a larger weight is chosen to represent the term in the functional. Figure 3c shows the difference between two different values of the weight. The selection of λ is based on the term's ability to keep the high resolution information contained in the divergence of the initial guess field while also maintaining the general pattern of the divergence of the climatology. These experiments in addition to the following two criteria allow for the selection of the weight. The value of λ is chosen to be ten times the weight of the ship data.

The second kinematic term describes the fit to the curl of climatology, and its weight is η. The term is similar to the divergence term in that its effects on
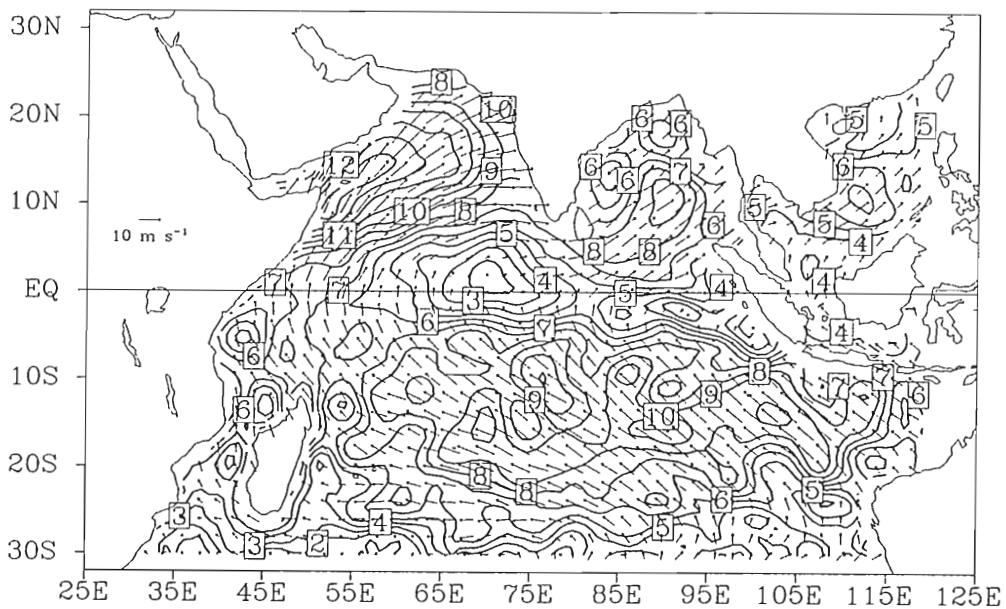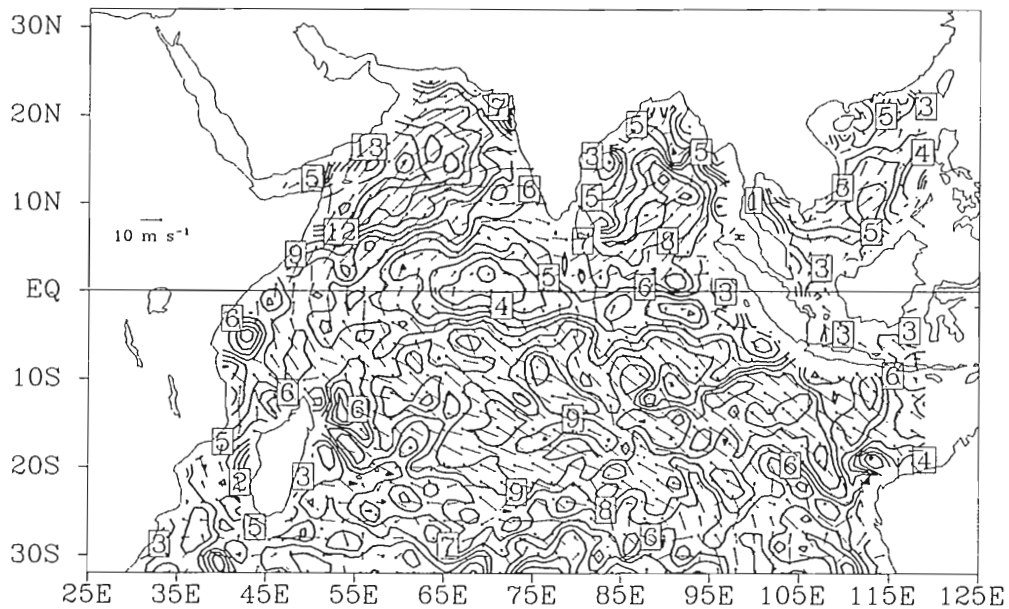
Figure 3b.   (Top) The initial guess for the period 7 July 1978 to 5 August 1978.
(Bottom) The results for the same period. The weights chosen are

Figure 3b.   (Top) The initial guess for the period 7 July 1978 to 5 August 1978.
(Bottom) The results for the same period. The weights chosen are
$\beta = 1, \delta = 10, \lambda = 1, \eta = 1$. The figure shows the ability of the
smoothing term to remove erroneous data and eliminate noise
from the field.

Figure 3c.   The divergence fields for the results for the period 7 July 1978 to 5 August 1978. (Top) The weights chosen are $\beta = 1$, $\delta = 1$, $\lambda = 1$, $\eta = 1$. (Bottom) The weights chosen are $\beta = 1$, $\delta = 1$, $\lambda = 10$, $\eta = 1$. The

22

Figure 3d. The curl fields for the results for the period 7 July 1978 to 5 August 1978. (Top) The weights chosen are $\beta = 1$, $\delta = 1$, $\lambda = 1$, $\eta = 1$.

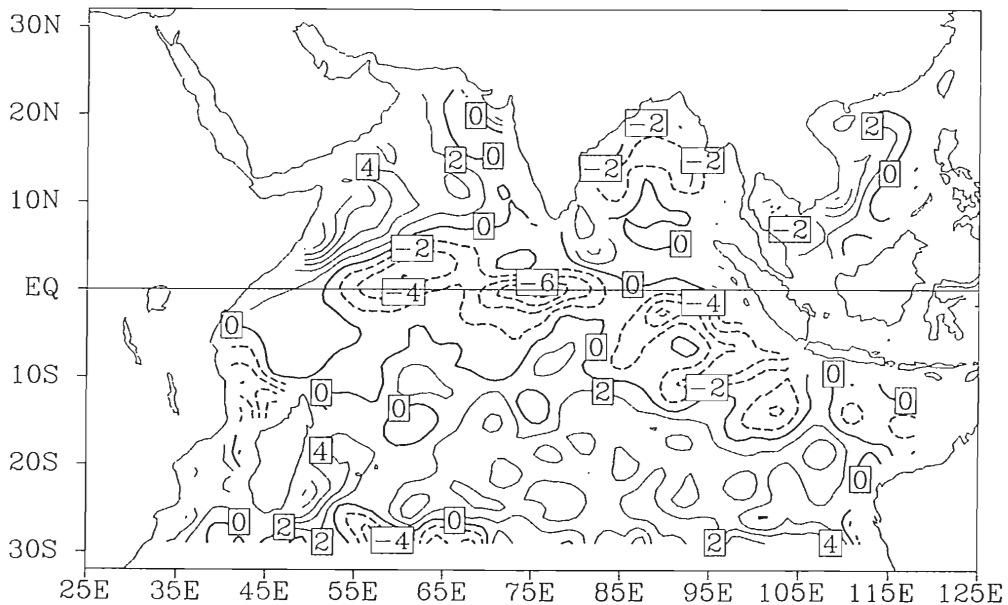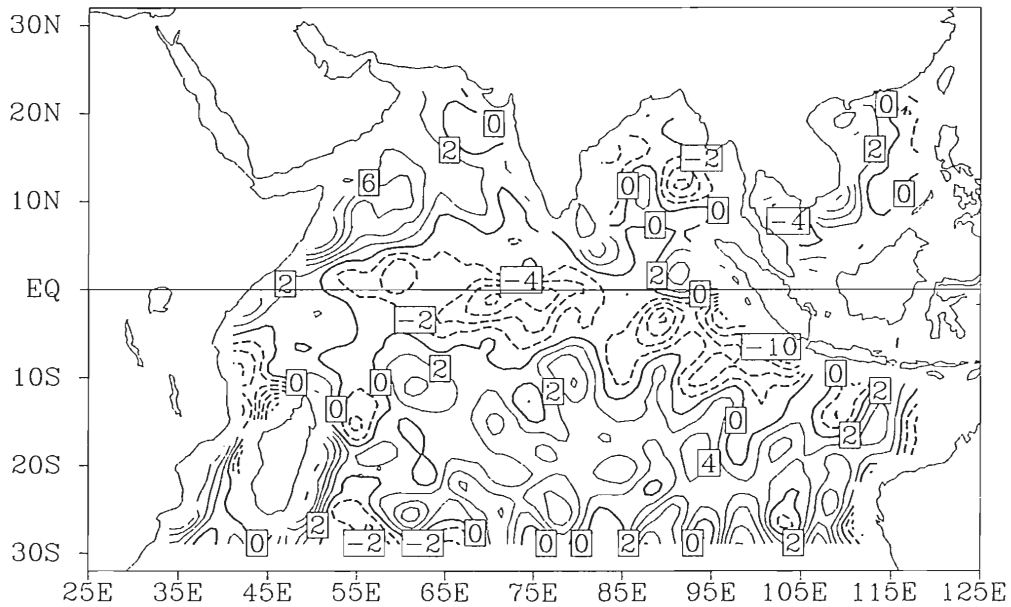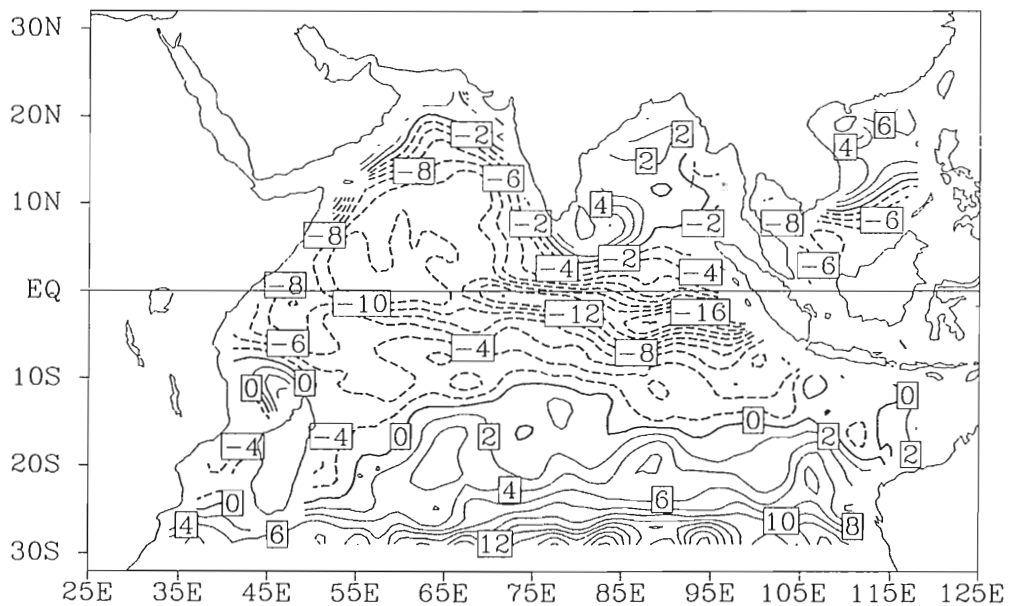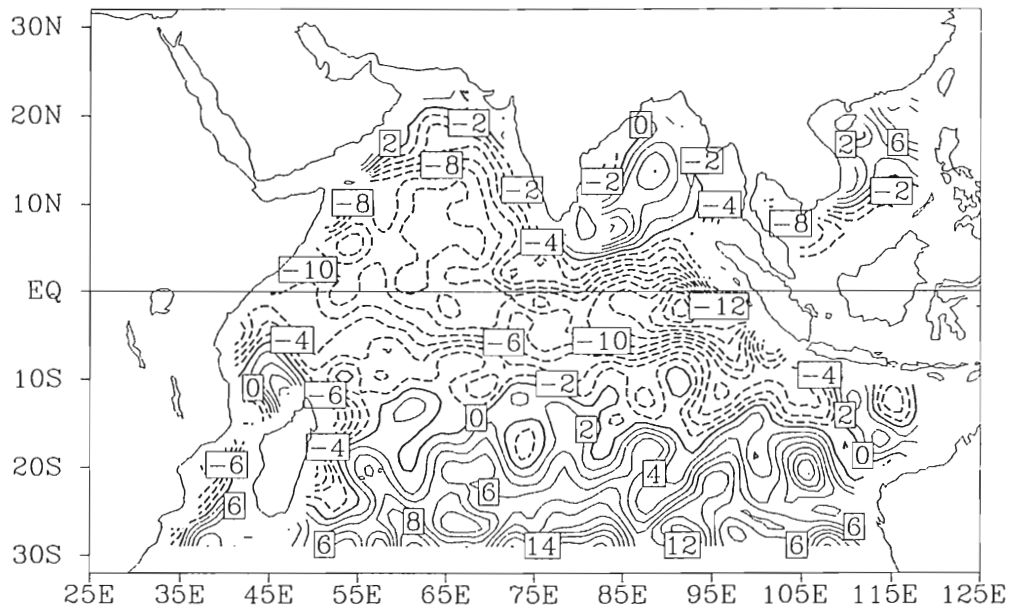Figure 3d. The curl fields for the results for the period 7 July 1978 to 5 August 1978. (Top) The weights chosen are $\beta = 1$, $\delta = 1$, $\lambda = 1$, $\eta = 1$. (Bottom) The weights chosen are $\beta = 1$, $\delta = 1$, $\lambda = 1$, $\eta = 30$. The figure shows the ability of the curl term to make changes to the curl of the resultant field.

the resultant field are subtle and that the results are not very sensitive to changes in the weight of the term. In order to understand its effects, the curl fields must be examined (figure 3d). Again, the weight is chosen for its ability to affect the curl field to the point where the initial guess field information is retained while maintaining the general climatological patterns of the curl field.

An additional method for selecting the optimal weights is one in which the minimization is required to recreate raw data that has been removed from the input field. This test is done to quantify various effects of weight selection on the resultant fields. In the data void test, the input ship data in a region of many ship observations is removed from the data file. Once the minimization is performed, the rms difference between the results and the removed data are calculated. In order for the data void test to be successful, the rms errors should be sufficiently small to allow for variation in the replacement of the winds. That is, the winds taken out of the minimization must be replaced by adequately similar winds. For this study, the region west of the southern tip of India is selected for the data void. For the period of 7 July to 5 August 1978, the ship data for a 2° by 2° box is removed and the minimization is performed. Adjustments are made to the weights to minimize the rms errors. A balance is sought between this method and those described earlier so that the local effects and the global effects of the weight adjustments are both taken into account. For the final selection of weights, the rms error for u and v for the 2° by 2° data void box are, $RMS_u = 1.57 \text{ m s}^{-1}$ and $RMS_v = 0.89 \text{ m s}^{-1}$. These rms errors are relatively small in magnitude compared to the average u and v of 7 m s^{-1} and 3.5 m s^{-1}, respectively, that had been removed from the region. It can be relatively small in magnitude compared to the average u and v of 7 m s^{-1} and 3.5 m s^{-1}, respectively, that had been removed from the region. It can be concluded that the estimation of the optimal weights are sufficient to fill in local data voids with valid data.

24

Table 1. Final selection of weights for the cost functional.

Weight	Term Represented in Functional	Weight Value
α	Fit to ship data	1
β	Fit to SASS data	1
δ	Laplacian	1
λ	Divergence	10
η	Curl	30

4. 2   30-day Results

The first results obtained from the minimization of the cost functional are those on the 30-day time scale. The weights for the ten and five-day results should not be adjusted because there is no climatology or truth upon which to base a change in the weights. If the weights are adjusted based on the monthly climatology, the ten and five-day information is easily smoothed or adjusted out of the results because they might be taken as erroneous information since they do not agree with climatology. Error associated with changes in the weights will be larger on the five-day time scale than they will be on the 30-day time scale because of the less reliable results. However, the local sensitivity errors which will be discussed in section 5 reveal very small errors in relation to the wind speed and therefore the same weights can be used for all of the time periods.

Calculation of the 30-day resultant fields yields three wind field maps that contain a few differences from the FSU climatological winds that are valid Calculation of the 30-day resultant fields yields three wind field maps that contain a few differences from the FSU climatological winds that are valid on the midpoint of each month (Figure 4). The figures show specific large scale regions where the climatology and 30-day results differ. The first two figures

show similar large scale regions of positive and negative difference. Notice the region of large positive values over the Arabian Sea monsoon with negative values near the African coast. These are associated with the different position of the maximum winds of the Findlater Jet in the results that is located to the southwest of the climatological position for most of the study period. The difference arrows in this region have little cross flow component and therefore show a general correspondence in same direction of the climatology and results. However, in the trade wind region, a large negative difference occurs due to the larger magnitude winds associated with the data. The cross flow component of the difference arrows in the trade wind region throughout the study period show that the climatology and results contain a direction difference as well. This shows that the results generally contain more of a northerly component than the climatology. A region of positive values and northerly difference arrows exists near Madagascar and is also a result of anomalous data values. The 30-day average resultant field contains much more of a strong southerly component that persists throughout the monsoon season. The region of noisy values across the 30°S latitude band is a result of the lack of sufficient data and the inability of the minimization to calculate accurate gradients at the boundaries. Therefore, the boundary does not contain useful synoptic information. Figure 4c shows an overall negative pattern signifying that the magnitude of the result winds are larger than the climatological winds. The trades continue to be stronger and have a more northerly component while the strong winds associated with the monsoon regions appear to be lasting longer than normal. The values are slightly larger than in figures 4a and b but still are strong winds associated with the monsoon regions appear to be lasting longer than normal. The values are slightly larger than in figures 4a and b but still are less than ten percent of the wind magnitude and are within limits of acceptable variability of the region.

Figure 4a.   Magnitude of the climatological winds minus the magnitude of the result field winds for the period 7 July to 5 August 1978. Contours are of m s^{-1}.

Figure 4b.   Magnitude of the climatological winds minus the

Figure 4b.   Magnitude of the climatological winds minus the magnitude of the result field winds for the period 6 August to 5 September 1978. Contours are of m s^{-1}.
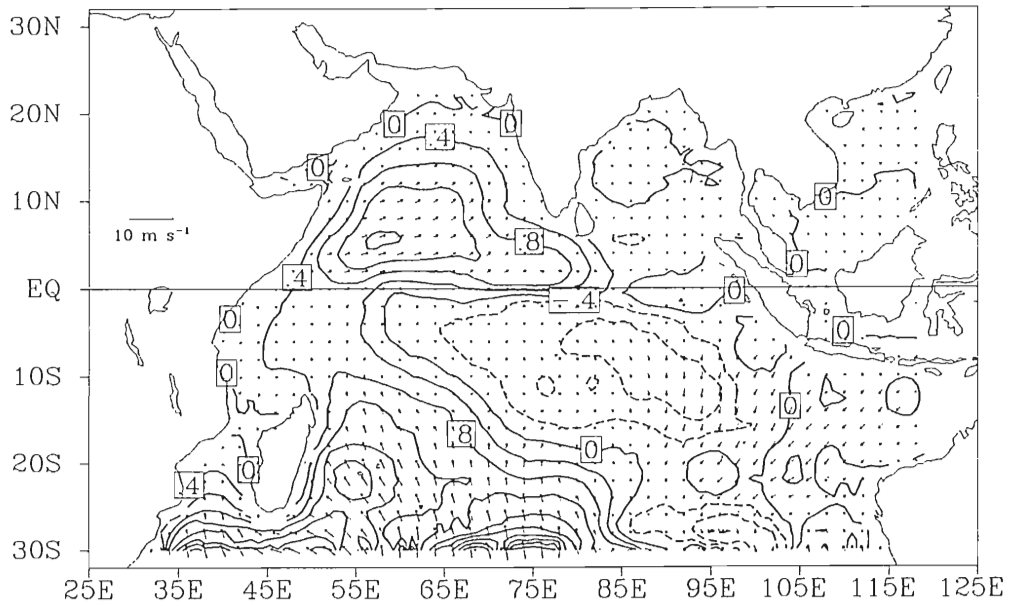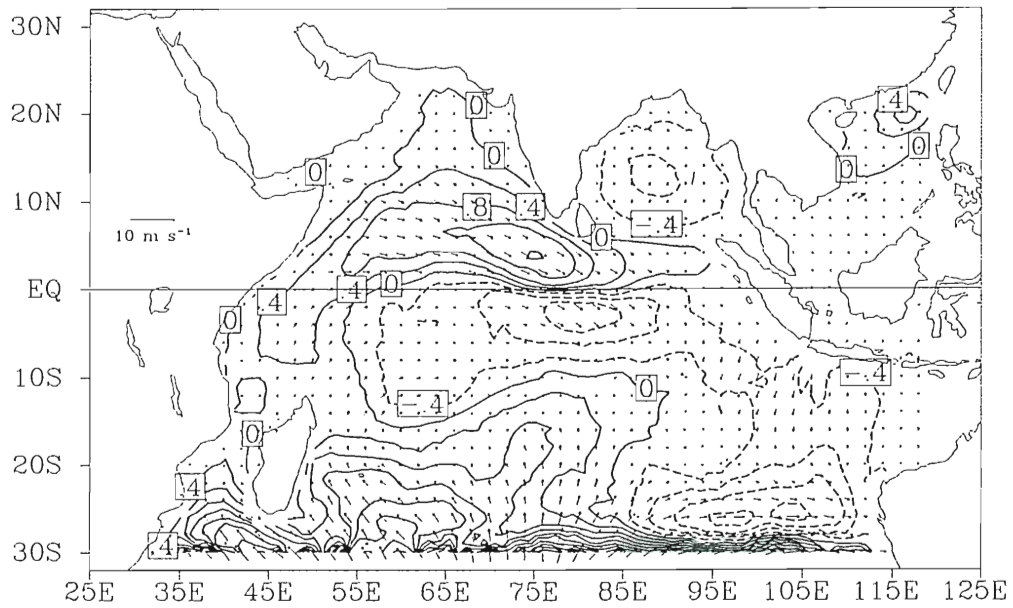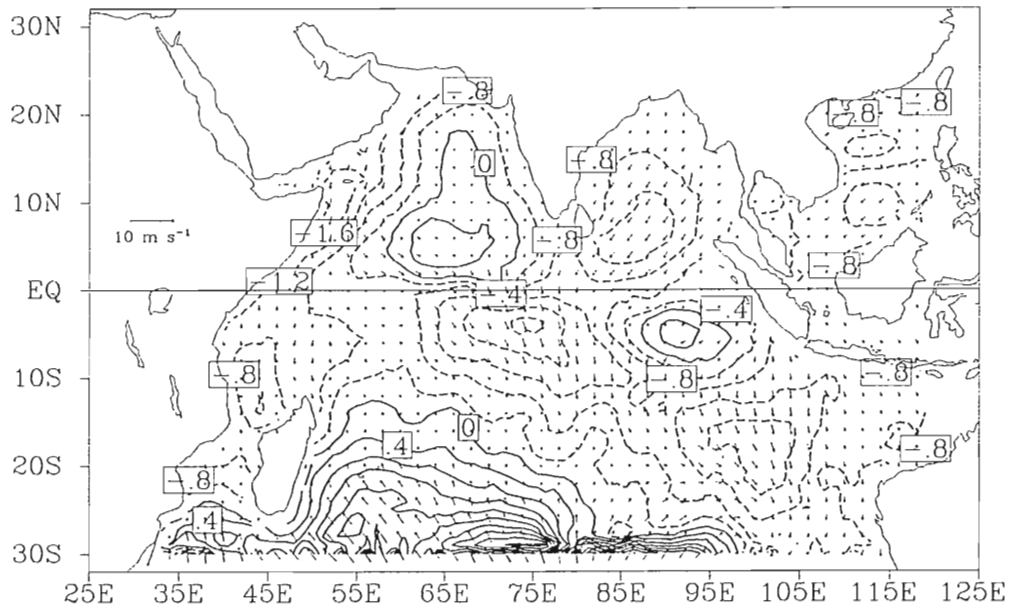
Figure 4c.   Magnitude of the climatological winds minus the magnitude of the result field winds for the period 6 September to 4 October 1978. Contours are of m s^{-1}.

4. 3   Ten and Five-day Results

As discussed previously, the weights for the 30-day results are determined and used for all resultant fields in the ten and five-day cases throughout the study period. In order to calculate the ten-day resultant field, the climatology used is the monthly FSU climatological winds interpolated the fifth day of the ten-day period. The ship and SASS data are ten-day averaged, instead of 30-day averaged. Any data voids in the input field (where no ship or SASS data are available) are filled with data from the previous ten-day period. The minimization of the functional for the ten-day data produces resultant fields for nine time periods (Figure 5). Note the position of the trade wind maximum in the southeastern Indian Ocean in figure 5 (top). This feature is different from the July climatology which shows two maxima; one in the east and one in the west. This ten-day result shows how the maximum lies in the east for the first half of the month and the west the second half (not shown), thus resulting in a monthly climatology that contains both maxima.

In order to calculate the five-day wind fields, each ten-day field is used as the climatology for the two five-day cases that it overlaps. The ship and SASS data are five-day averaged. The results of the minimization are shown in the Appendix (Section 7). A comparison of the 30, ten, and five-day resultant fields shows overall consistency with slight differences due to the diminishing confidence of the averaged ship and SASS data. An additional comparison can be made by averaging three ten-day resultant fields and comparing them to the appropriate 30-day resultant field. For the three comparisons that can be made, be made by averaging three ten-day resultant fields and comparing them to the appropriate 30-day resultant field. For the three comparisons that can be made, small differences appear in the first 30-day period with no coherent pattern. In the following two periods large differences occur in the three monsoon regions;

the Arabian Sea, the Bay of Bengal, and the South China Sea. This is a result of the data being weighed less and less by number of observations as the minimization is performed on smaller time scales due to the fewer observations. It says that the minimization on shortening time scales, using data with less and less confidence, becomes more like the climatology used for that time period.

Each of the eighteen five-day resultant fields will now be examined with emphasis on six areas of interest. The first region of examination is the southeast trades; next will be the region east of Madagascar, termed the Mascarene High (Rao *et al.* (1978); the third area is the Bay of Bengal monsoon region; then is the South China Sea region, followed by the Arabian Sea monsoon region. Finally, the region of small magnitude winds over the equator just south of the Arabian Sea monsoon region from 60°E to 80°E, termed the equatorial minimum, is examined.

Throughout the monsoon season on the monthly time scale, the most consistent winds in speed and direction are the southeast trade winds in the Southern Hemisphere (Hastenrath and Lamb (1979)). However, the five-day time scale wind fields reveal much about the shorter time scale variation of these winds. Already pointed out is the movement of the speed maximum during the month of July from west to east. The magnitude of the trades also appears to strengthen and weaken during the monsoon season. In the month of August and in late September, the normally well defined region of maximum winds becomes very disorganized and several local maxima are discernible. In early September, the maxima almost disappear as a large region of similar magnitude winds prevail.

Perhaps associated with some of these changes are the fluctuations in the region of the Mascarene High. The winds in the region east of Madagascar,
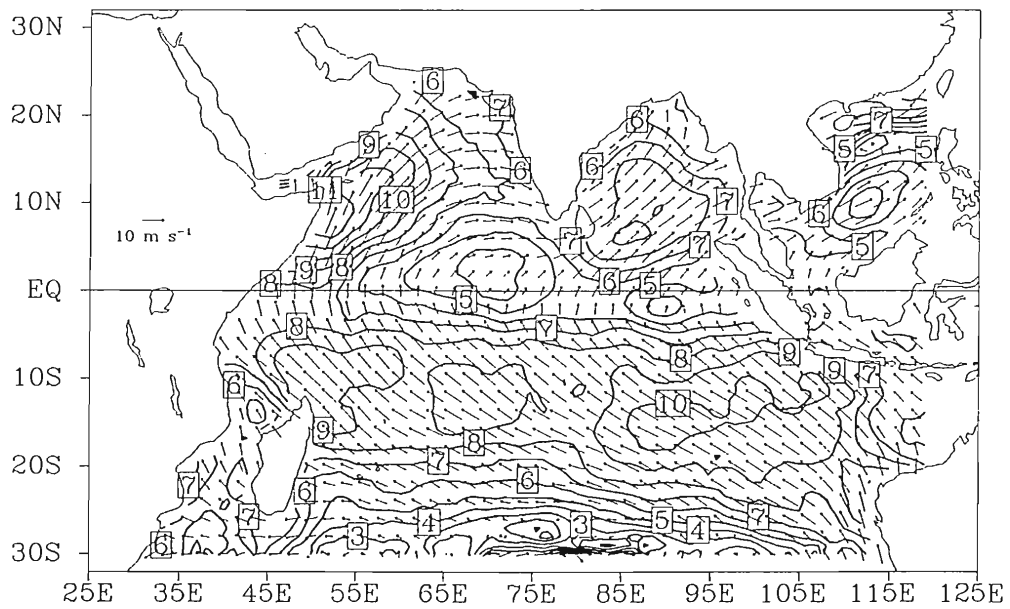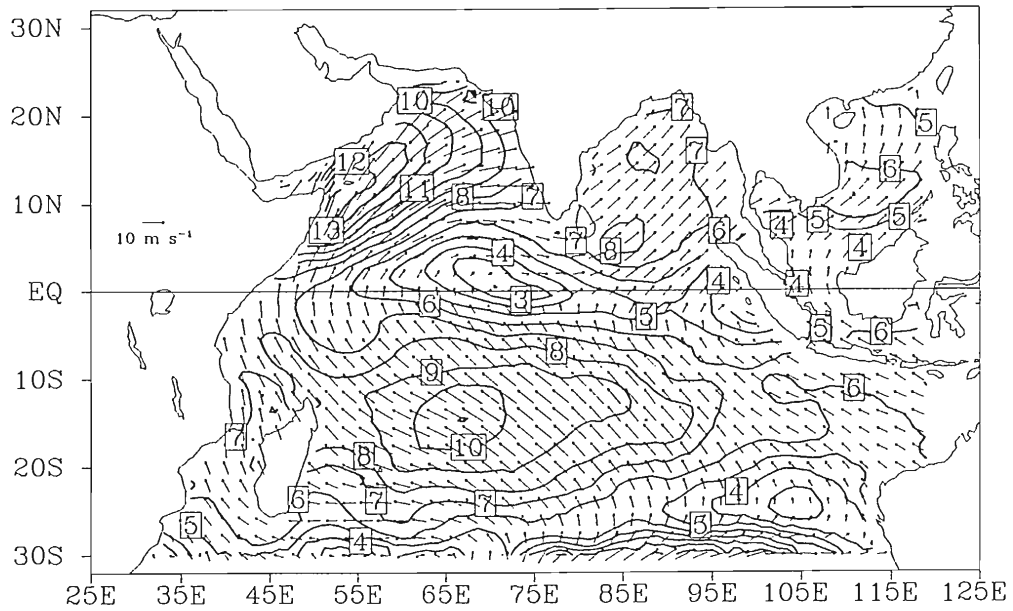
31

Figure 5.   The resultant field for two ten-day cases; (top) 7 July to 16 July 1978 and (bottom) 15 September to 24 September 1978.

from 26°S to 18°S, are variable on the five-day time scale. The winds flow steadily for 10 to 25 days and then abruptly slow, creating a large area of convergence east of Madagascar. These winds then become strong and northerly. This occurs at three irregularly spaced times during the study period. Of course, one of the contributing factors to the large fluctuations in the wind field may be the fact that the region contains very few data and hence is sampled inadequately during the study. If data are obtained only once or twice during the five-day period, the observation may be for one specific local event rather than a large region of variability. Upon examination, it is seen that the the data in the region rather than the minimization itself is the cause of the fluctuations in the wind field.

Another region of interest is the Bay of Bengal region, characterized primarily by steady southwest winds. The monsoon season of 1978 in the Bay of Bengal contains mostly stronger winds, spatially and temporally, than either the FSU climatological winds or Hastenrath and Lamb (1979), but with only small fluctuations. In early to mid September, the monsoon reverses and the region contains interesting features that cannot be distinguished on monthly time scales. The winds over the Bay of Bengal split into two distinct patterns. The northern pattern is one in which the winds decrease in magnitude and reverse, while in the south, a wind maximum continues.

This splitting of the winds into two distinct patterns is also seen in the South China Sea region. This region contains the most anomalous winds from climatology in this study. The winds in July of 1978 are consistent with expected July winds except are larger in magnitude. However, as August climatology in this study. The winds in July of 1978 are consistent with expected July winds except are larger in magnitude. However, as August begins, the winds quickly decrease in magnitude and reverse in the northern part of the region by late August (Figure 6). This earlier than normal reversal

and subsequent strengthening represent large variations from typical monthly climatology. As these winds continue through the remainder of the study period, a strong line of north-south convergence is stationary near 20°N.

The last two regions of variability are crucial for measuring the strength of the monsoon season. On the five-day time scale, the Arabian Sea monsoon, i.e. the Findlater Jet (just east of the African coast), has consistently strong winds with small five-day variability. The position of the Findlater Jet can determine which regions of India may be hardest hit with monsoon rainfall (Hastenrath (1991)). The intensity of the cross equatorial wind flow also determines the cross-equatorial water vapor transport. The mean position of the Findlater Jet may vary from season to season, but the jet position also changes during the season (Rao *et al.* 1978, 1981). This movement is illustrated in Figure 7 and more specifically in Table 2. There are only seven different locations at which the core of the jet (defined as the grid point with the largest wind speed) is found during this study. The movement of the jet core is limited to a small area. It tends to move to the south and west during the course of the season and moves quickly to the north after the maximum winds have occurred and the winds begin to reverse (Figure 2). Notice that the last four to six positions in the table correspond to times during the transition to the winter monsoon where the Findlater Jet is very weak and almost indiscernible. The position of the jet maximum is consistently slightly south and west of the mean July position found in Rao *et al.* (1978). The position of the entire jet itself, however, is consistent with Hastenrath (1991). The intensity of the jet is, however, inconsistent with climatological intensity. The average magnitude of the consistent with Hastenrath (1991). The intensity of the jet is, however, inconsistent with climatological intensity. The average magnitude of the resultant field jet core during the first 40 days of the summer monsoon is 16

m s^{-1}, which is one to two m s^{-1} greater than the climatological winds given in Hastenrath and Lamb (1979.)

The final region of interest is the equatorial minimum region. This region is comprised of winds that are generally smaller than climatology in magnitude with the center of weak winds to the north of the FSU winds climatological position. This region is a secondary indicator of the amount of moisture brought north from the Southern Hemisphere oceans. The magnitude of the average winds in and around this minimum is proportional to the influx of moisture from the southeast trades. Since the magnitude of the winds in the region is generally smaller than those of climatology, the influx of moisture would appear to be less than normal. As shown in Figure 8, the monsoon season of 1978 produced near average rainfall over India. Perhaps the combination of a stronger than normal Findlater Jet and a weaker than normal equatorial minimum may have produced a normal flux of moisture across the equator to provide the near normal rainfall over India. The average wind speed across the western half of the equatorial Indian Ocean over the entire analysis period is relatively small and constant, with the minimum weaker and centered slightly to the north of the normal position

In summary, 30-day averaged wind fields are calculated and examined for differences from climatology. These differences are determined to be a consequence of the intramonsoonal variability of the data. Ten-day averaged resultant fields are calculated and used as climatology for five-day fields in order not to dispose of the short time scale information contained in the data. The five-day results show much variability in the Indian Ocean region. The order not to dispose of the short time scale information contained in the data. The five-day results show much variability in the Indian Ocean region. The magnitude of the southeast trade winds changes as the maximum moves from the east to the west. The Mascarene High region winds have an interesting

decrease in magnitude just before the winds become strong northerly. The three monsoon regions; Bay of Bengal; South China Sea; and Arabian Sea; each contain jet-like features of convergence that have much five-day variability. The equatorial minimum contains secondary information about the cross equatorial flow of the monsoon season.

Table 2. The Position and Wind Magnitude of the Core of the Findlater Jet.

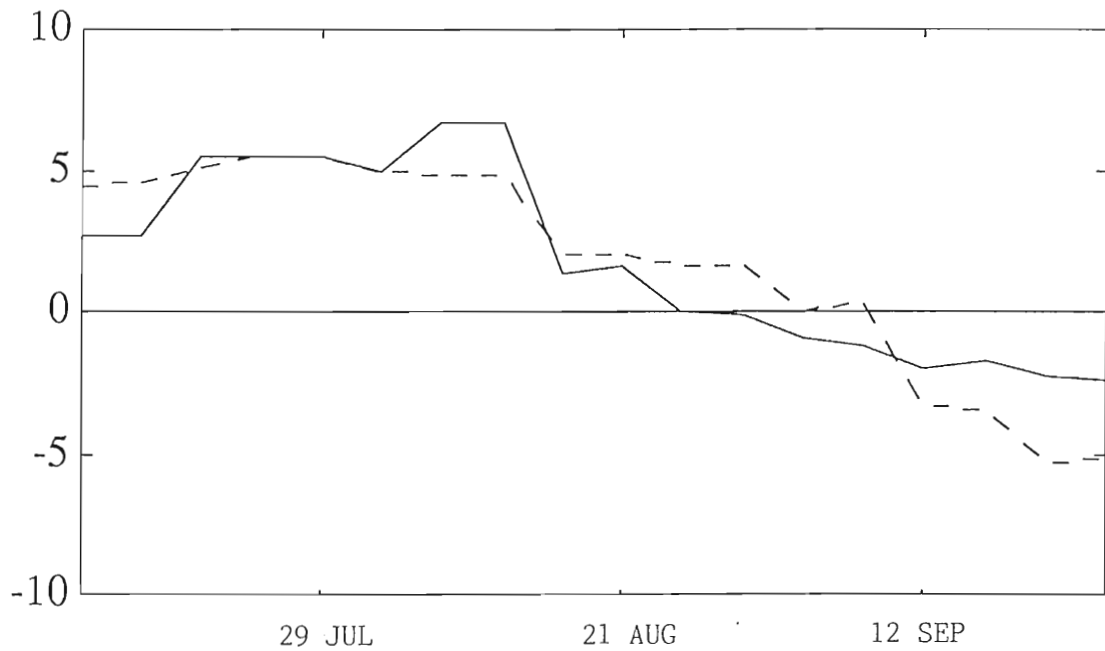| Longitude (°E)	Latitude (°N)	Magnitude (m s^{-1})	Letter in Figure 7
56	13	16.51	A
56	13	14.90	A
56	13	15.90	A
54	11	16.85	B
53	11	16.47	C
53	11	15.22	C
54	11	16.05	B
53	11	16.09	C
52	9	14.29	D
53	9	15.45	E
52	9	14.37	D
52	9	13.76	D
52	9	9.91	D
52	9	10.90	D
46	12	8.51	F
47	13	7.71	G
46	12	11.35	F
46	12	11.69	F
46	12	11.35	F
46	12	11.69	F

Figure 6.   The average u (solid) and v (dashed) components of the averaged
             wind speed of the South China Sea monsoon region (5°N to 25°N,
             105°E to 120°E) for each five-day resultant field during the course

             of the monsoon season (7 July to 4 October 1978). The values
             given are in m s^{-1}.
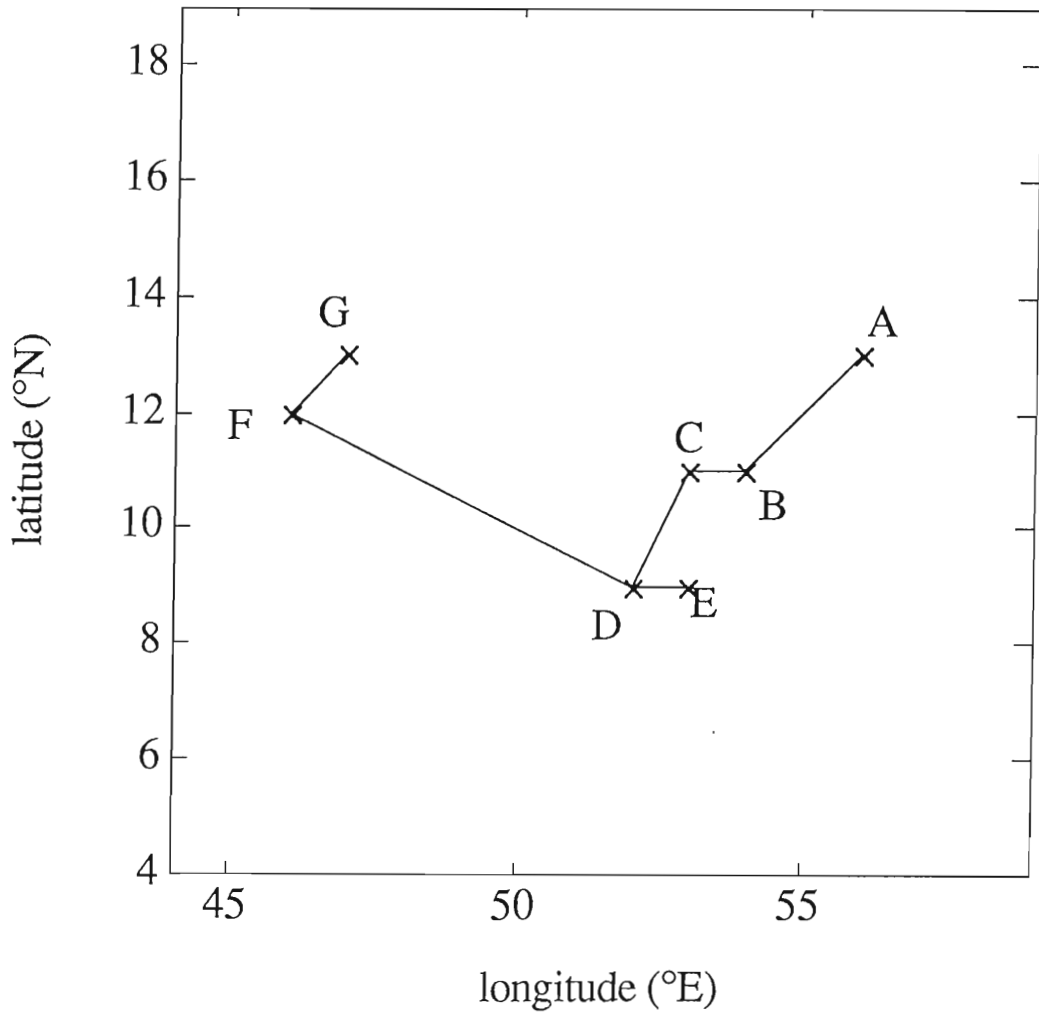
Figure 7.   The position of the Findlater Jet during the course of the monsoon

Figure 7.   The position of the Findlater Jet during the course of the monsoon season (7 July to 4 October 1978). The letters correspond to values given in Table 2.
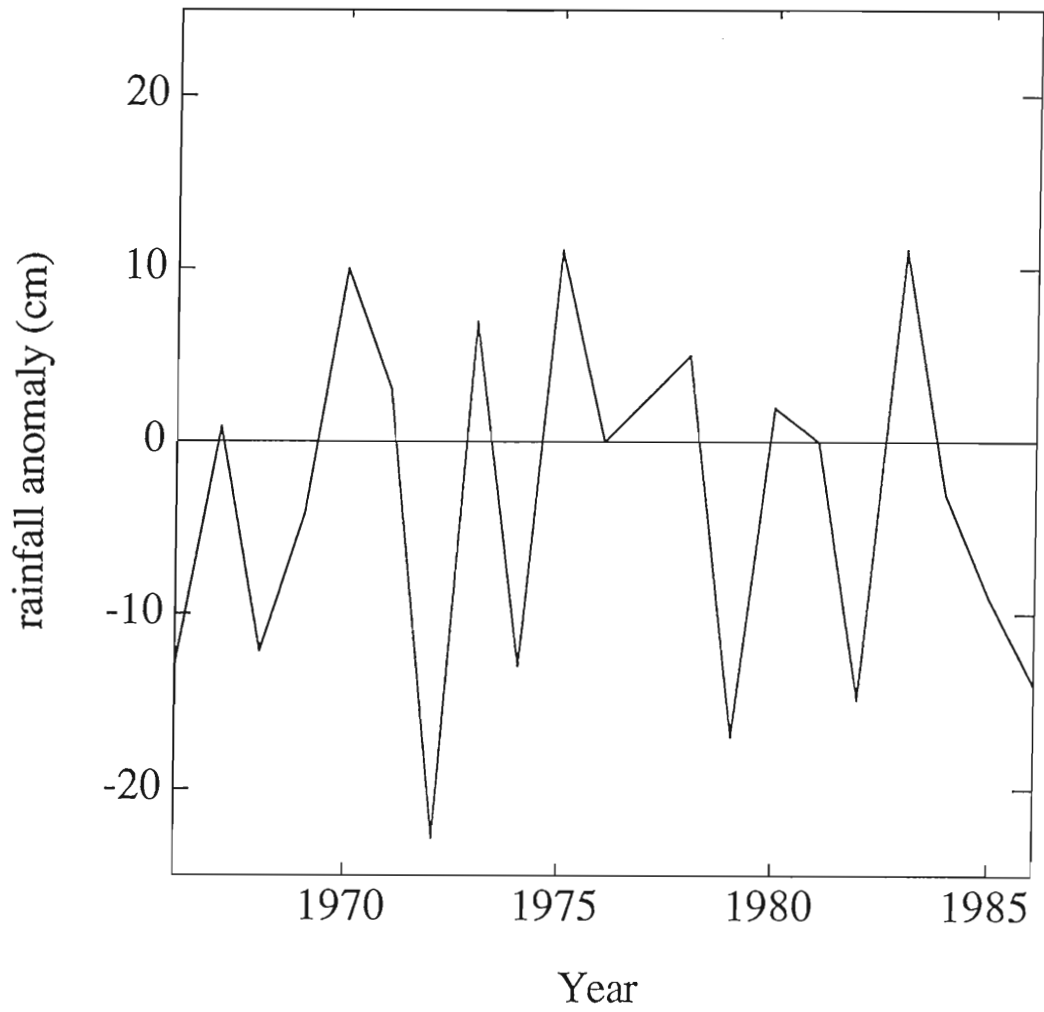
Figure 8.   The departure from average rainfall for each summer monsoon
season (June, July, August) in centimeters (from Yasunari (1991)).

5. Sensitivity Analysis

5.1 Response Functions and Sensitivity Parameters

Selecting the optimal weights associated with each term of the cost functional is difficult since the true wind field is not known for comparative purposes. However, information about the optimal weights can be obtained by knowing how much, and in which areas, the terms are sensitive to changes in the weights. Even though the weights are not spatially dependent, regions of the Indian Ocean can be affected differently. The relative magnitude of the weight depends on how sensitive the solution is to the weight. Smaller adjustments are made to the weights depending on specific areas of the field revealed by the analysis which need better representation. One way to determine sensitivity is by first specifying a scalar response function that is representative of the solution. This allows the sensitivity of thousands of points to be approximated by a single scalar quantity. This response function will change with the weights and should be based on its pertinence to the resultant fields. For simple quantities such as winds, response functions that are given by the curl (in s^{-1}) or kinetic energy (in $m^2\,s^{-2}$) of the field is considered. The equations for these two response functions are,
energy (in $m^2\,s^{-2}$) of the field is considered. The equations for these two response functions are,

for the curl response function, $R_c = \sum_{i,j} \left(\hat{k} \cdot \vec{\nabla} \times \vec{V}(i,j) \right)$ (1)

and for the kinetic energy response function,

$$R_e = \sum_{i,j} R_1 + R_2 = \sum_{i,j} \left(u(i,j) \right)^2 + \left(v(i,j) \right)^2 \qquad (2)$$

where,

$$R_1 = \left(u(i,j) \right)^2 \quad \text{and} \quad R_2 = \left(v(i,j) \right)^2$$

A sensitivity parameter for each weight, S_w, is defined as the change in the response function for two different weight selections results divided by the change in the weight, w. In practice these variations are measured by adjusting the weight ± 0.5 % of the selected weight. The small increment is taken to ensure an accurate calculation of the derivative. The normalized sensitivity parameter is given by the equation,

$$S_w = \frac{w \, \Delta R}{R \, \Delta w}$$

where the Δ is the change in the value for a ± 0.5% change in the weight. The weights in Table 1 are considered as the center of the variation of the weights. The response function for each of the results is determined using equations 1 and 2 and then the sensitivity parameter, S_w is calculated for each. The sensitivity parameters for the two different response functions are given in Table 3.

given in Table 3.

Table 3. Sensitivity Parameters of the Two Response Functions for Each of the Four Variable Parameters.

	Parameter Value	Sensitivity Parameter (S_{we})	Sensitivity Parameter (S_{wc})
β	1	0.0067	0.024
δ	1	-0.022	-0.018
λ	10	0.0085	0.0089
η	30	0.013	-0.012

These sensitivity parameters denote the ability of the weight to affect the response function. A positive sensitivity parameter indicates an increase in R_e or R_c with an increase in the weight. A negative parameter indicates that the increased (decreased) weight results in a decrease (increase) in the appropriate response function.

The SASS weight, β, has the smallest and the largest values of the sensitivity parameters R_e and R_c, respectively. The SASS term is designed to smooth and enhance the more reliable ship data. It does not change the kinetic energy of the resultant field much because it is not very different from the initial guess field. Although it does not drastically change the results, the SASS term does affect R_c much more, due to the effect of curl built into the solutions of the SASS data as they were dealiased. Since the satellite swaths involve large areas of observations, all of the data are taken into account when dealiasing and curl of the solution is a factor in

into account when dealiasing and curl of the solution is a factor in determining the solution. Therefore, the SASS data automatically contains smoother than normal curl values.

The smoothing weight, δ, is large and negative in both of the response functions. Increased smoothing has the expected effect of decreasing the overall magnitude of the winds since the magnitude of each wind is directly connected with its neighboring winds. This smoothing will decrease the total kinetic energy and spatial derivatives of the wind field. Therefore, the average curl of the field will also decrease.

Changes in the divergence weight, λ, have a small effect on both of the response functions. This is consistent with the earlier statements that the two kinematic constraints require large changes to affect the resultant field. The value with respect to R_c is consistent with Legler *et al.* (1989), which found that changes in the divergence term weight had little effect on the curl field.

The curl term weight, η, has very different effects on the two response functions. The sensitivity parameter value for R_e is very similar to the value for the divergence weight for the same reasons as above. The effect on the curl field is negative due to the adjustments made during the minimization toward climatology. The effect is not very large compared to the other parameters but is larger than its kinematic counterpart. This is probably due simply to the response function used. If the response function were average divergence rather than average curl, the values of the parameters of the two kinematic terms would likely be reversed.

The important sensitivity parameters to examine are those for the smoothing term and the curl term with respect to R_e, and the smoothing term and the SASS term with respect to R_c. These appear to have the largest smoothing term and the curl term with respect to R_e, and the smoothing term and the SASS term with respect to R_c. These appear to have the largest effect of the respective response functions although all terms need to be examined for more specific local effects.

5.2 Local Absolute and Relative Sensitivity

The sensitivity parameter values show the overall sensitivities of the results to changes in the weights. In order to see any local effects of changes in the weights, local absolute and relative sensitivities must be calculated. For the curl response function, the derivative of the response function with respect to the weight is calculated. The local absolute sensitivity (LAS) of R_C at the point (i, j) is given by the simple equation,

$$LAS_c(i, j) = \frac{\Delta R_c(i, j)}{\Delta w} \tag{3}$$

For the kinetic energy response function, R_e, the derivative of each of the two components of the function, R_1 and R_2 is taken with respect to the weight, i.e. the local absolute sensitivity (LAS) of R_e, is given by the equation,

$$LAS_e(i, j) = \left[\left(\frac{\Delta R_1(i, j)}{\Delta w}\right)^2 + \left(\frac{\Delta R_2(i, j)}{\Delta w}\right)^2\right]^{1/2} \tag{4}$$

In order to determine the relative dimensionless sensitivity, the absolute sensitivity is normalized by multiplication of equation 3 and 4 by the weight divided by the response function. The local relative sensitivity (LRS) of R_C is determined by normalizing equation 3. The local relative sensitivities for R_e are determined similarly. The LRS for both of the response functions are not very useful in representing the sensitivity field.

response functions are not very useful in representing the sensitivity field. Values of the energy or curl at or near zero cause the normalized relative sensitivities to become extremely large. These areas tend to dominate the

44

sensitivity field and outweigh the other areas. The sensitivity values are true, but because they are relative changes, small values of the energy or curl can be associated with tremendous relative changes but negligible absolute changes. Instead, emphasis in this study will be placed on the absolute sensitivities.

The LAS values are shown for the two response functions in Figures 10 through 13. Since these are absolute changes in different units, their magnitudes are difficult to compare. Note that there is a relationship between the sensitivity fields of the two different response functions chosen here (see Meyers *et al.* (1992)). The curl fields are related to the spatial derivatives of the energy field, so maxima in the energy field correspond to zero lines in the curl field.

Another relationship among the sensitivities is that similar patterns are found in the sensitivities of R_C for the three terms involving climatology. In general, the patterns in the sensitivity of the curl response function are nearly identical for each of the three terms. This is a result of the fact that each of the terms involve fits of the derivatives of the results to derivatives of climatology.

The LAS's of both response functions of the SASS term, weight β, in Figure 9 show the result that the highest sensitivities are over the open ocean where there are few ship observations. This is expected because the minimization actually has only two data sets to fit the results to in these areas of sparse ship data. High sensitivities in both response functions also occur west of Australia. One particular area where the value of R_e is low areas of sparse ship data. High sensitivities in both response functions also occur west of Australia. One particular area where the value of R_e is low and the value of R_C is high is the equatorial region from 70°E to 90°E. This is due to the large curl values generated by the directionally varying but small
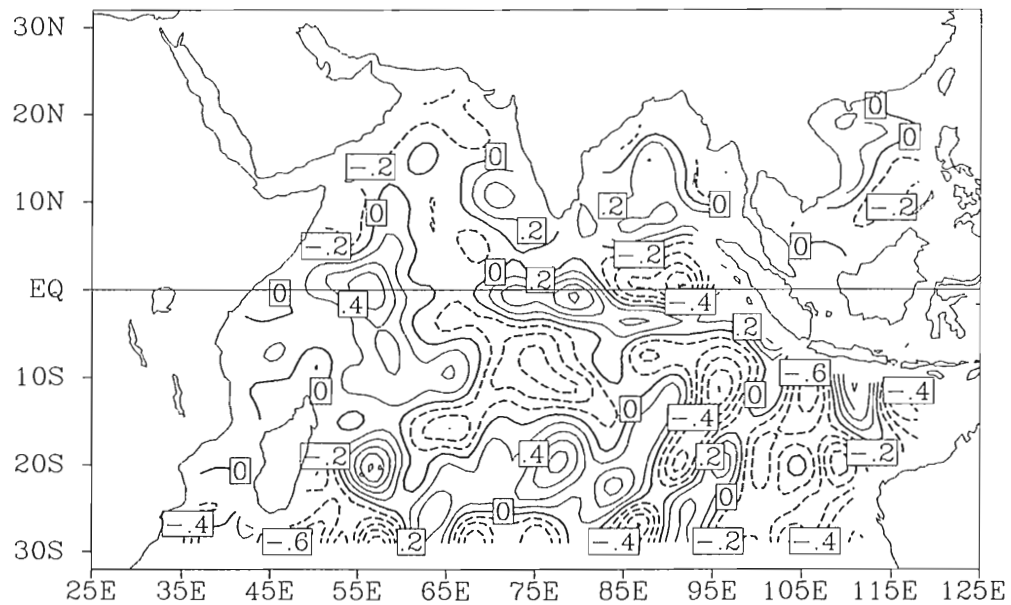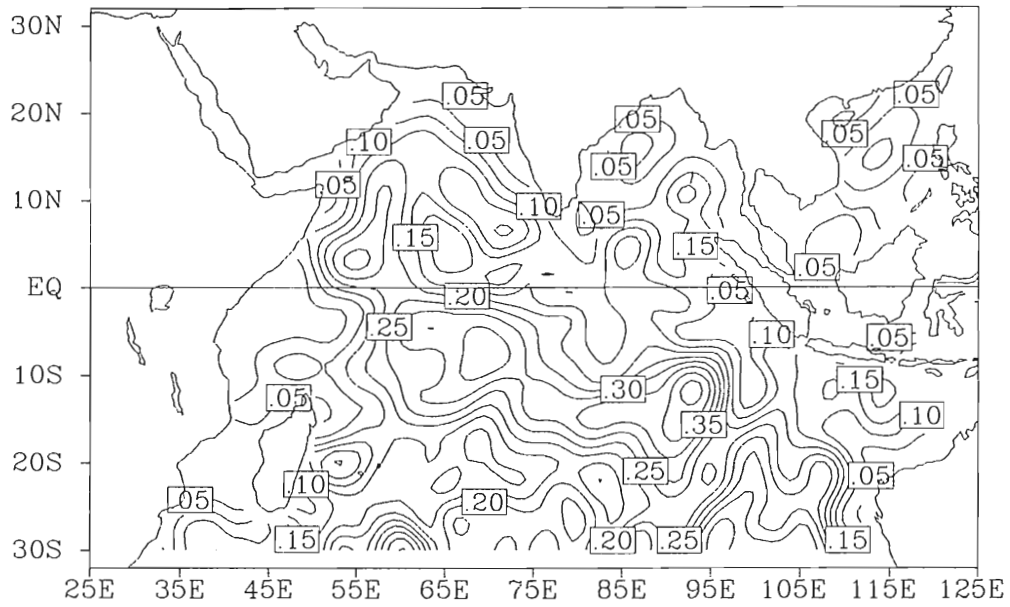
Figure 9. (Top) The Local Absolute Sensitivity (LAS) for R_e of β during

Figure 9. (Top) The Local Absolute Sensitivity (LAS) for R_e of β during the period 7 July to 5 August. Units are $m^2 \; s^{-2}$. (Bottom) LAS for R_c. Units are $10^{-6} \; s^{-1}$.

wind magnitude solutions.

The LAS of the smoothing term, weight δ, (Figure 10) shows regions of very high sensitivity where data are initially erroneous or where the result winds are very different from climatology. Recall that the smoothing term measures the lack of fit of the Laplacian of result winds minus climatology. Large differences of the resultant field from climatology will cause the term to make larger adjustments in the wind solutions during the minimization. Therefore, varying the weight of the term causes high sensitivity in these regions.

The LAS of the divergence term, weight λ, (Figure 11) is very small in both response functions and is similar to the smoothing term in that the regions of largest sensitivity correspond to regions where the climatology and resultant fields differ the most. The patterns for the LAS of R_c are much smaller than other terms due to the lack of ability of the divergence term to affect the curl field. The LAS of R_e however reveals the regions where large differences between climatology and results occur.

Figure 12 shows the two LAS's for the curl term, weight η. The sensitivity of this term for R_e is very small in regions of small curl and the region west of Sumatra, where the curl is a maximum, shows very high sensitivity. The curl response function contains information related to the derivative of R_e. The equatorial regions contain large values of curl and hence are the areas in which R_c is at a maximum.
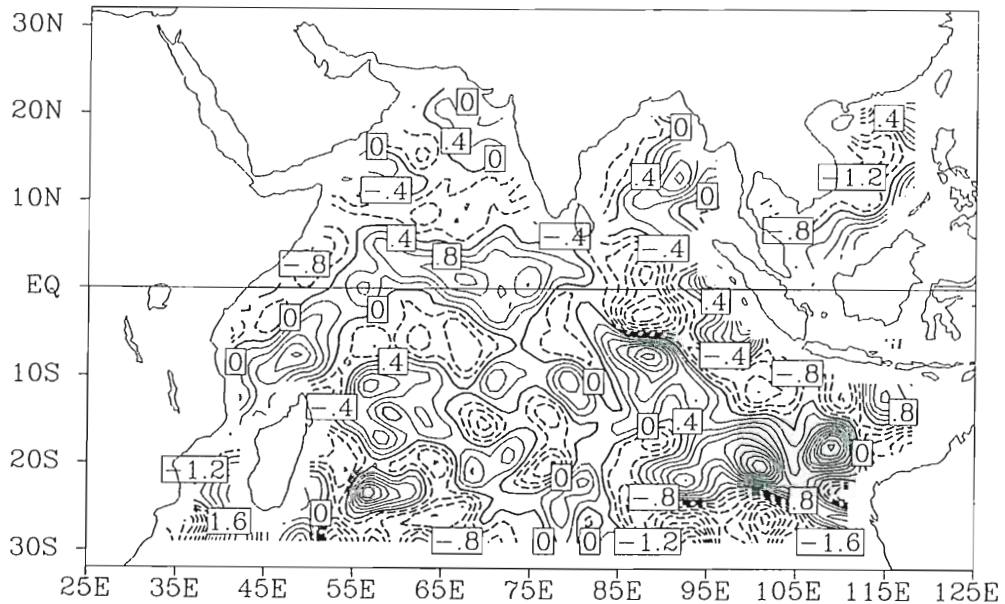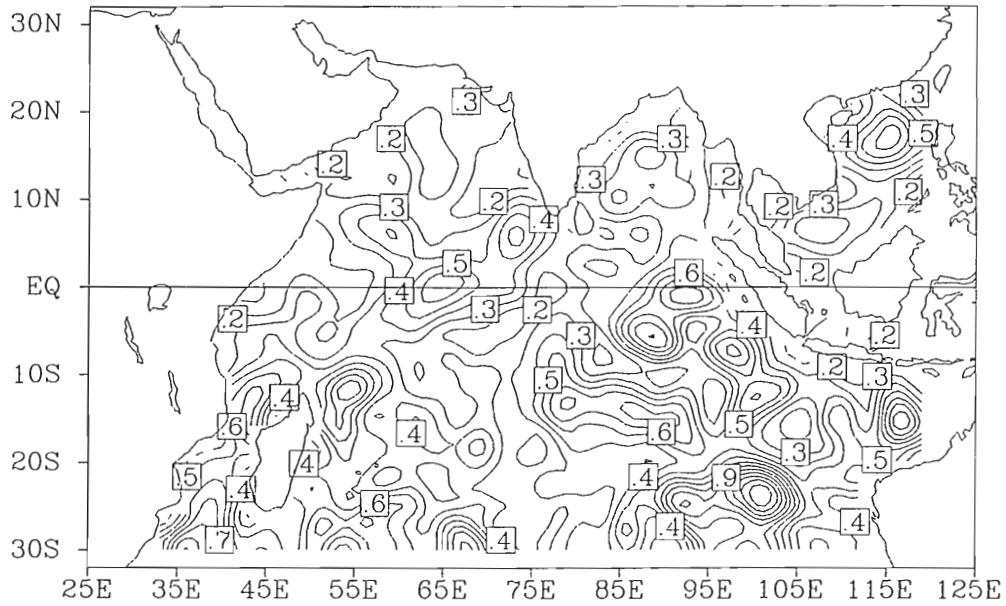
Figure 10.   (Top) The Local Absolute Sensitivity of δ for R_e during the
period 7 July to 5 August. Units are $m^2 s^{-2}$. (Bottom) LAS for

Figure 10.   (Top) The Local Absolute Sensitivity of δ for R_e during the
period 7 July to 5 August. Units are $m^2 s^{-2}$. (Bottom) LAS for
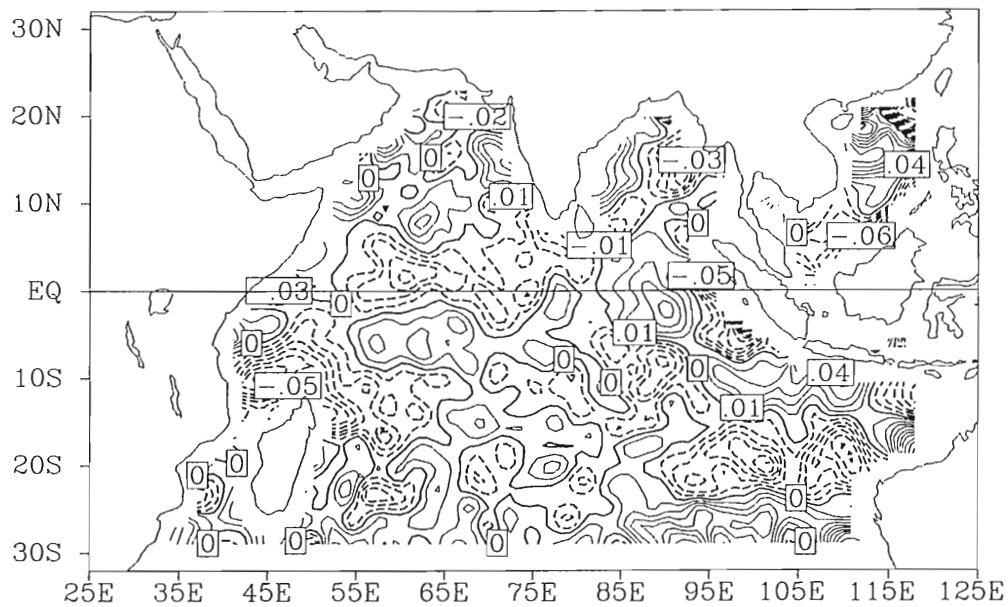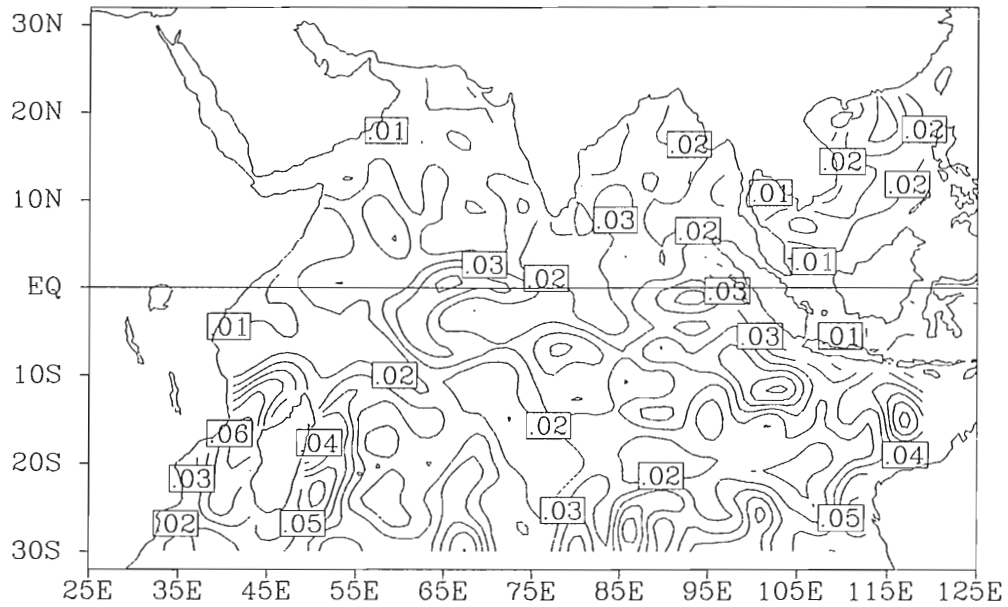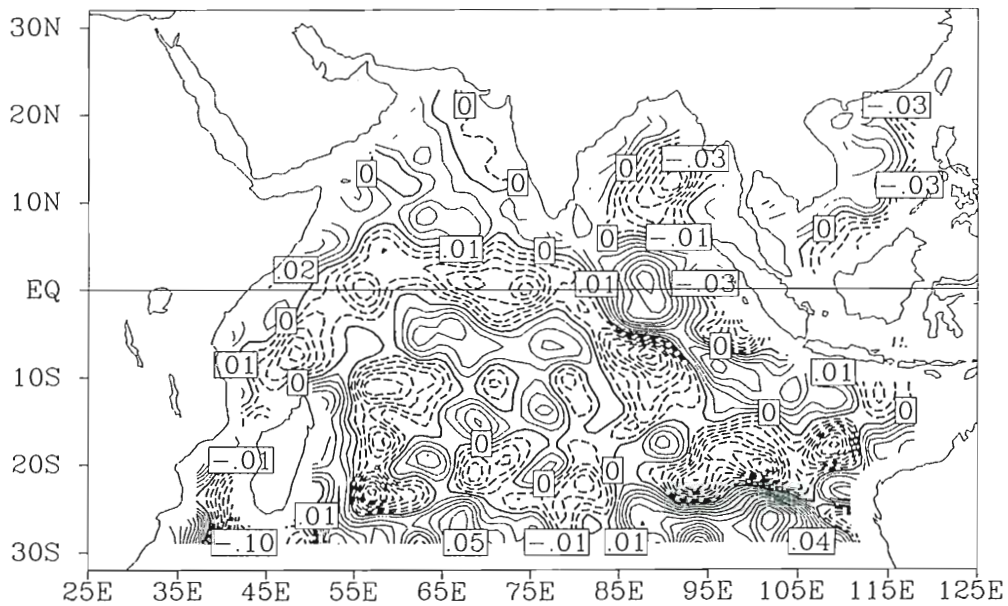R_c. Units are $10^{-6} s^{-1}$.

48

Figure 11.   (Top) The Local Absolute Sensitivity of λ for R_e during the
             ~~period 7 July to 5 August. Units are m^2 s^{-2}. (Bottom)LAS is for~~

Figure 11.   (Top) The Local Absolute Sensitivity of λ for R_e during the
             period 7 July to 5 August. Units are m^2 s^{-2}.   (Bottom)LAS is for
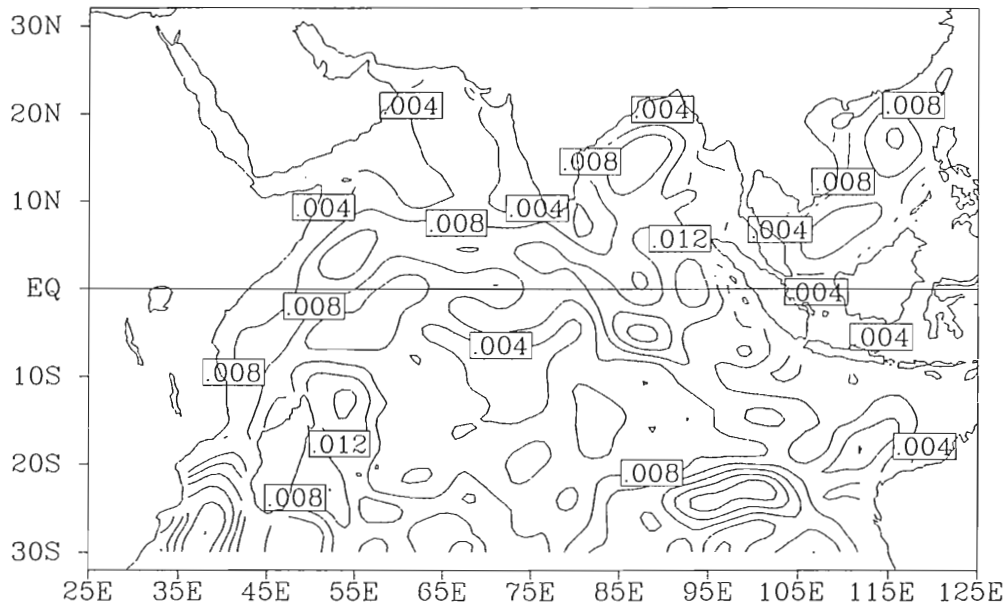 R_c. Units are 10^{-6} s^{-1}.

Figure 12. (Top) The Local Absolute Sensitivity of η for R$_e$ during the period 7 July to 6 August. Units are m^2 s^{-2}. (Bottom) LAS is for R$_c$. Units are 10^{-6} s^{-1}.

5.3 Local Sensitivity Error

Since the selection of the optimal weights is based on many different experiments and some subjective decisions, it is important to know the magnitude of the errors as a function of weight uncertainty. A type of root mean square error can be determined from the changes in the resultant fields with respect to weight changes. In order to calculate the local sensitivity error (LSE), the selected optimal weights are varied plus and minus ten times their calculated sensitivity parameters, S_w. Since there are four variable parameters, eight different variations of the weights are performed. An equation for the LSE at each point is given by the equation,

$$LSE(i,j) = \left(\frac{1}{8}\right) \sum_{k=1}^{8} \left[(u_k(i,j) - u_0(i,j))^2 + (v_k(i,j) - v_0(i,j))^2 \right]$$

where u_0 and v_0 are the wind components of the results with the optimal weights. The wind components of each of the eight different variations are represented by u_k and v_k. As stated above, the LSE is similar to an rms error due to weight uncertainty in the functional. The LSE field is shown in Figure 13. The average value of the LSE is slightly less than 0.1 m s^{-1}. So for a 10% error in the selection of the weights, the results are in error by approximately 0.1 m s^{-1}, and the maximum is 1.4 m s^{-1}. These errors can be compared for different areas of the Indian Ocean. An area such as the trade winds region may contain average wind speeds of 10 m s^{-1}. Hence small errors in weight selection do not appear to be significant in most areas of the winds region may contain average wind speeds of 10 m s^{-1}. Hence small errors in weight selection do not appear to be significant in most areas of the Indian Ocean. The LSE also helps to show why the same weights can be

used for each of the different periods in the study. There is less certainty in the results at the five-day time scale but since the number of observations are weighted, the ship and SASS data terms are smaller than on the 30-day time scale. Therefore, the climatological terms are relatively larger. Small adjustment might need to be made from one period to the next due to these data density differences, but the LSE is so small that making adjustments in the weights does not create a large difference in the results.

In summary, the sensitivity analysis performed in this study is helpful in determining the impact of each of the terms in the cost functional. Information is supplied through sensitivity parameters and local sensitivity that enables a determination of result error from weight uncertainty. The analysis is one way to examine the effects of each of the weights. It shows that the very sensitive smoothing weight tends to decrease the magnitude of the winds and the average curl of the field. The less sensitive SASS term adds information to the initial guess over the open ocean in the trade winds. The kinematic terms contribute more information in some areas than others and require much higher values than the data terms or the Laplacian term in order to effect change in the results because this analysis shows that their parameters are not as sensitive. Each of the terms and their weights in the functional has a crucial role in the resultant field. The sensitivity analysis identifies and helps to quantify that role. The sensitivity analysis helps to narrow the problem of multiple weights to perhaps one or two more influential weights so that more concentration may be placed upon these. The effects of weight uncertainty weights to perhaps one or two more influential weights so that more concentration may be placed upon these. The effects of weight uncertainty are also determined through rms type error analysis in order to determine areas and causes of large errors.
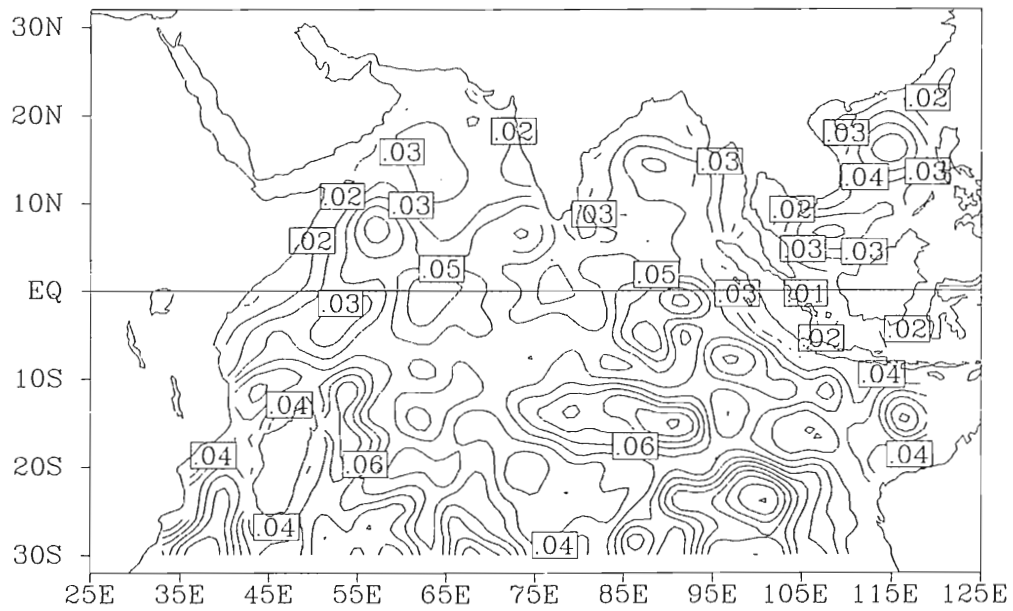
Figure 13.   The Local Sensitivity Error during the period 7 July to 5 August. Units are m^2 s^{-2}.

6. Summary and Conclusions

The combination of satellite and conventional ship data provides an opportunity to examine the Indian Ocean wind field variability that neither data source can provide alone. The COADS CMR5 ship observations tend to be concentrated in shipping lanes and very seldom can be confidently averaged over short time scales in certain regions of the Indian Ocean. The SEASAT scatterometer data provides limited but more evenly spaced coverage. However, it also contains biases and errors under certain conditions. The ship and SASS data are combined with information from climatological winds to demonstrate a minimization technique that provides short time scale wind fields on a one-degree grid.

The success of this technique depends on the determination of the proper cost functional discussed in section 3 and the selection of the best possible weights for each term of the functional as discussed in sections 4 and 5. The weights for the terms are selected by adjusting the weights and observing the changes in the result, divergence, and curl fields. These adjustments are compared to ship averages and determined if the change is beneficial to the results. The sensitivity analysis and the data void test are incorporated into the test criteria to determine overall sensitivity and local effects of the changing of the weight.

incorporated into the test criteria to determine overall sensitivity and local effects of the changing of the weight.

The sensitivity analysis is performed to determine the importance of each of the weights as well as any local effects that the terms have on the results. The analysis is accomplished by analyzing the change in two different scalar response functions which represent a basin-wide characteristic with respect to an alteration of each weight. These sensitivity parameters reveal the amount of change that occurs in the results as the weights are changed. Local sensitivities are calculated and show specific regions where terms are most influential and guide further adjustments of the weights. As a final calculation, the local sensitivity errors are determined. These errors are root mean square errors that represent the uncertainty of the results with respect to uncertainty in the weights (according to the sensitivity parameters). These errors are found to be much less than one percent of the magnitude of the winds at any given location in the study region for a ten percent change in the weights. These small errors show how a slightly incorrect determination of the weights leads to a very small variation of the results.

Results of the minimization reveal much about the five-day variability of the monsoon region. Areas where intramonsoonal variability are evident include the position of the Findlater Jet, the location of the maximum winds in the trades, the position and magnitude of the equatorial minimum, and the orientation of the winds over the South China Sea. The features are verified in the sensitivity analysis as regions of high sensitivity in the weights associated with fits to climatological data. This is due to large differences between the actual data, to which the results should be similar, in the weights associated with fits to climatological data. This is due to large differences between the actual data, to which the results should be similar, and climatological fields. The three terms involved attempt to put these differing data sets together and therefore make larger adjustments to the

results in these regions of large intramonsoonal variability. This does not say that the terms containing fits to climatology are not necessary in the functional or that they dominate the results. The adjustments made to the weights is simply to balance the known patterns contained in the climatology with the desired information contained in the ship and SASS data. The high sensitivity of some of the terms helps to point out specific areas in which important variability of the monsoon region occurs.

The conclusion can be made that the results show definite ability of the minimization technique to combine the raw satellite and ship data of the Indian Ocean with a information from a climatology to create short time scale gridded wind fields. In regions of sufficient data, the results are quite good compared to other studies in the past that denote the changing of position and orientation of features discussed here (Rao *et al.* 1978; Legler 1992). Difference fields calculated in section 4 show specific regions of result minus climatology maxima and minima. These regions reveal stronger than normal trade winds and intramonsoonal variability of the Findlater Jet. From the results however, it is seen that regions that lack adequate ship or SASS data tend to have high variability from one five-day period to the next which results in poor representation of synoptic scale features on the five-day time scale. This is found in the extreme southern portion of the study region and was also examined in the Mascarene High region. These areas of sparse data coverage are found to cause high sensitivities and large local sensitivity errors. In addition, the sensitivity analysis is useful in determining the importance of each functional term to the results and local sensitivity errors. In addition, the sensitivity analysis is useful in determining the importance of each functional term to the results and enabling the optimal weights to be selected. It can also be concluded that this technique for determining five-day wind fields can be used with current

ERS-1 scatterometer data rather than SASS data. Unfortunately, due to problems with this data, it became unavailable for this research. Future work in this area will examine this data as well as any improvements in ship or climatological data.

7. Appendix

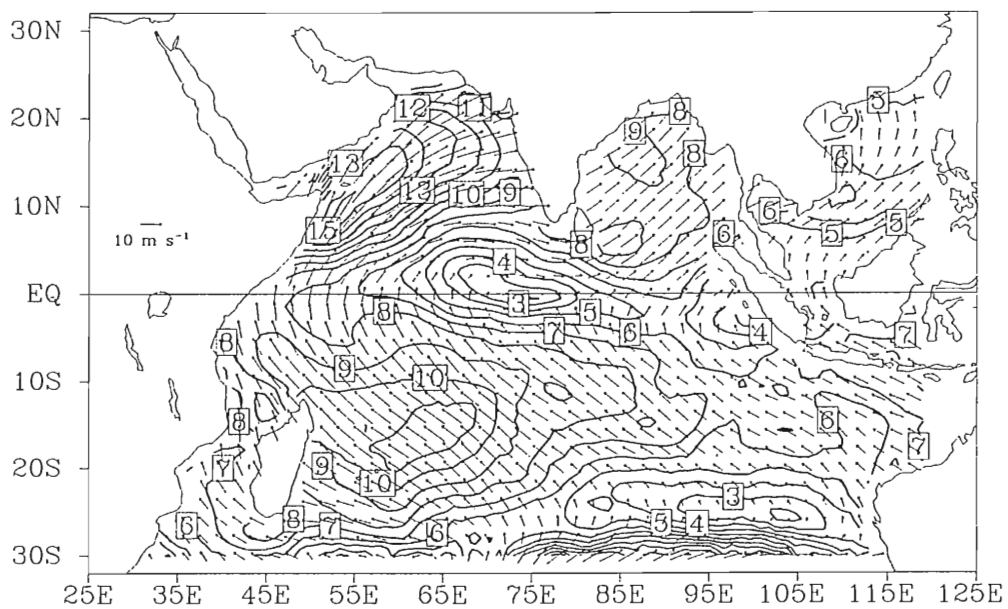Five-day resultant fields for the study period 7 July to 4 October 1978

Figure 14.   Resultant field for the period 7 July to 11 July 1978. Contours

Figure 14.   Resultant field for the period 7 July to 11 July 1978. Contours
are vector magnitude (in m s^{-1}). Directional arrows are drawn
at every other grid point.
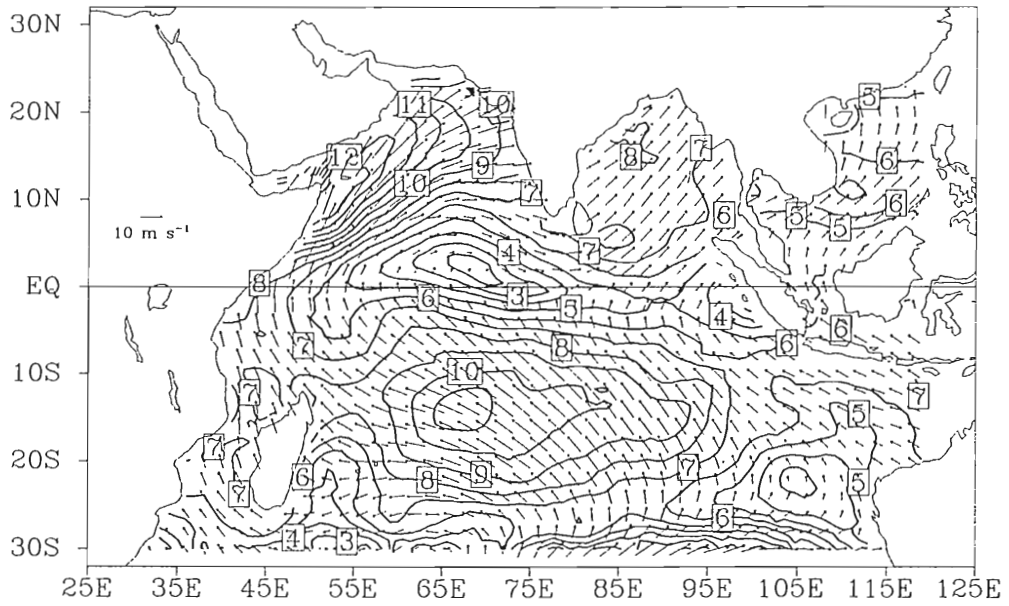
Figure 15.   Resultant field for the period 12 July to 16 July 1978.
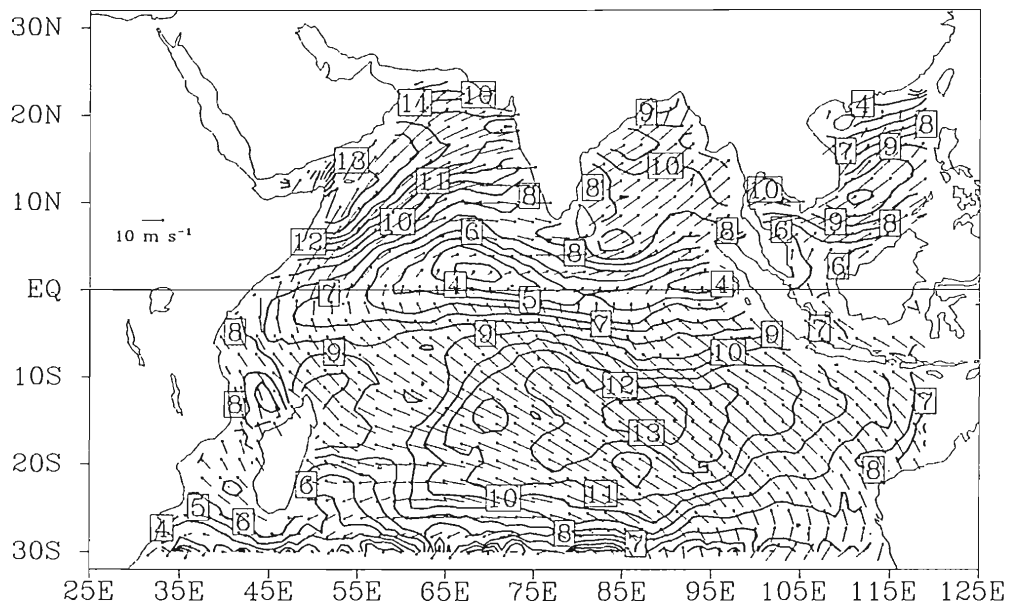
Figure 16.   Resultant field for the period 17 July to 21 July 1978.
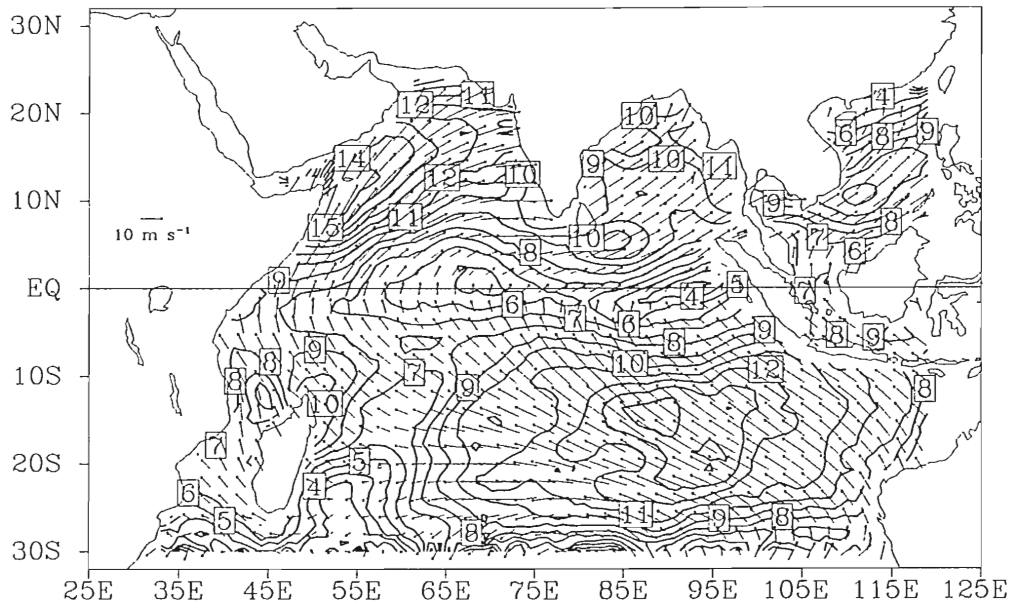
Figure 17.   Resultant field for the period 22 July to 26 July 1978.
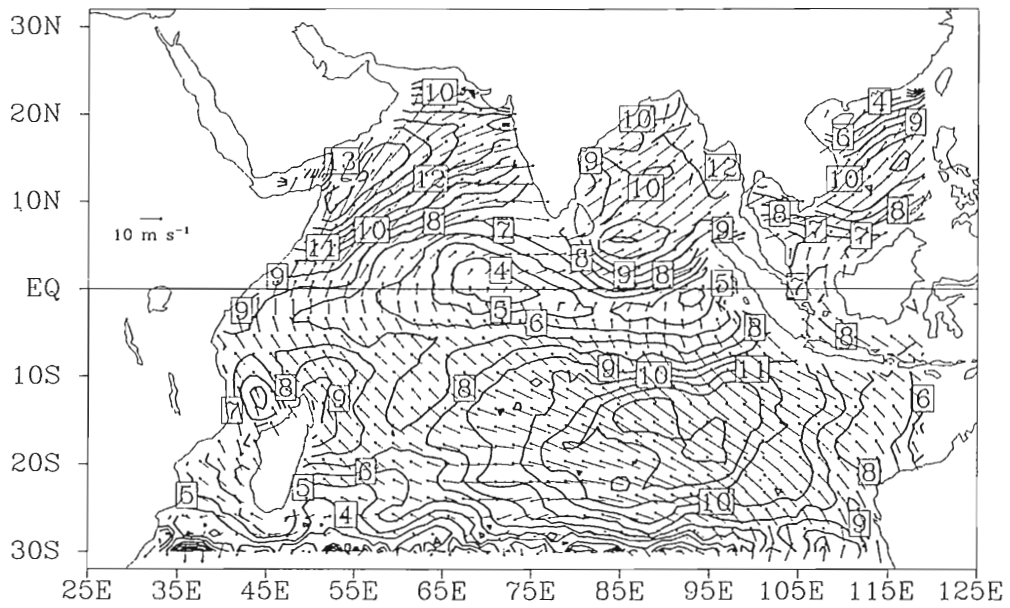
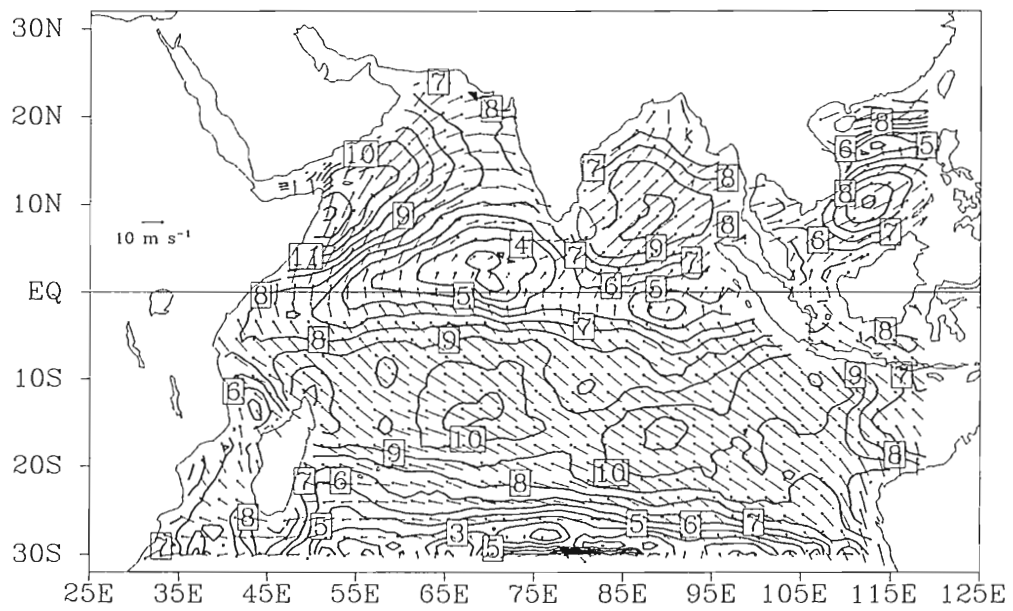Figure 18.   Resultant field for the period 27 July to 31 July 1978.
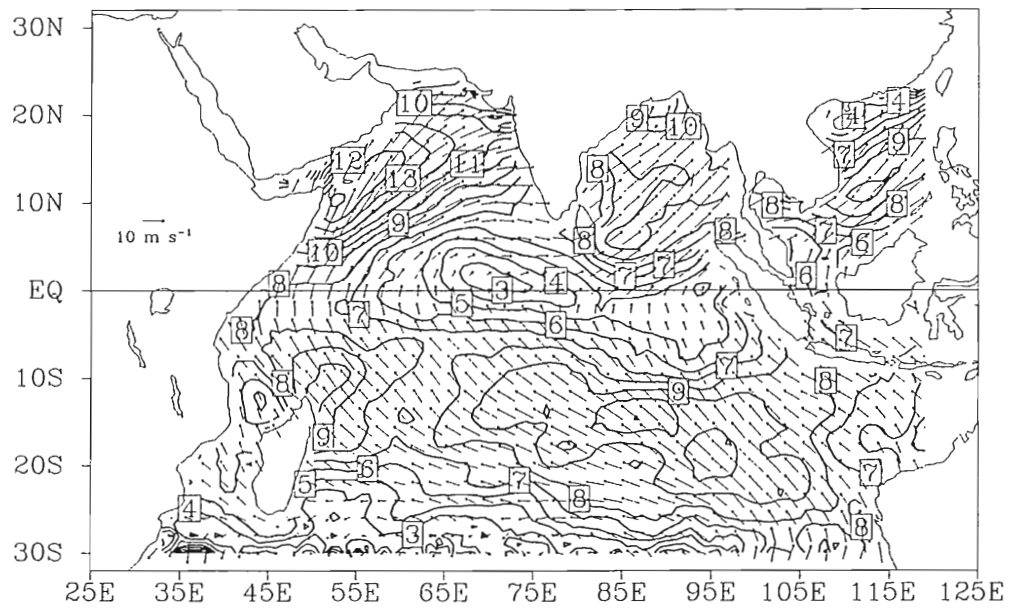
Figure 19.   Resultant field for the period 1 August to 5 August 1978.
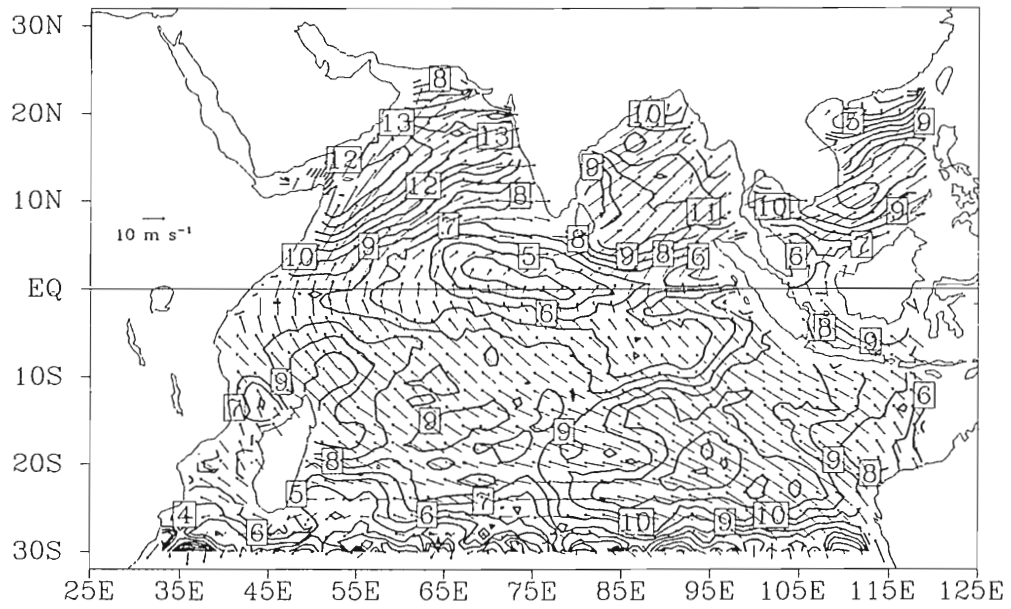
Figure 20.   Resultant field for the period 6 August to 10 August 1978.
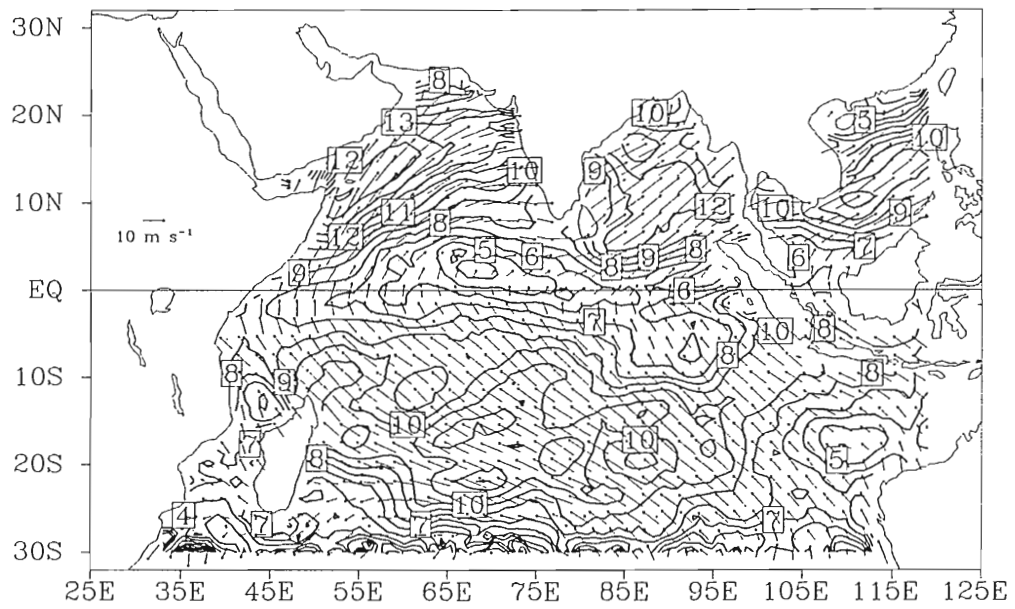
Figure 21.   Resultant field for the period 11 August to 15 August 1978.

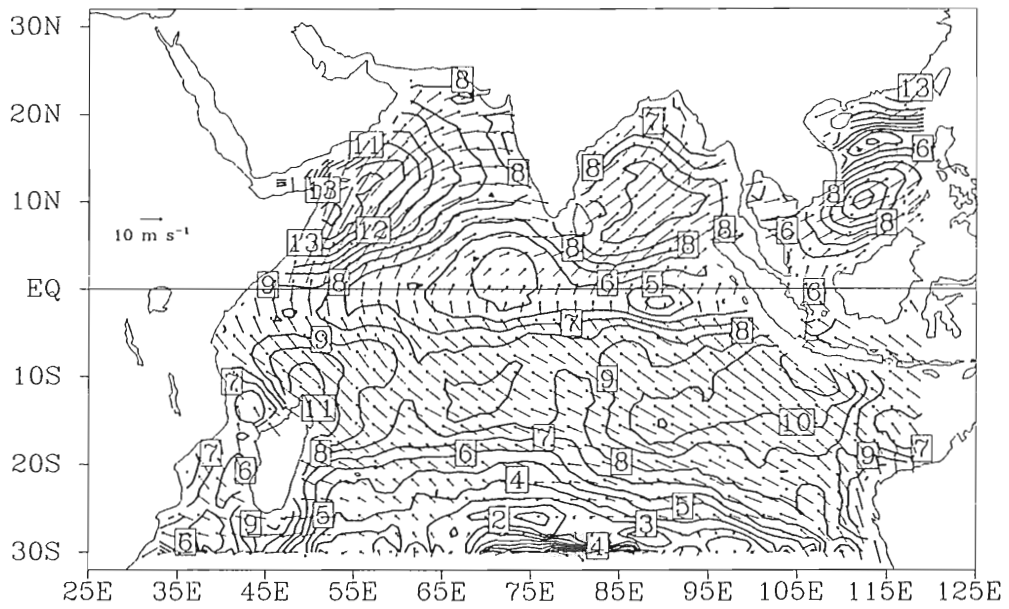Figure 22.   Resultant field for the period 16 August to 20 August 1978.

Figure 23.   Resultant field for the period 21 August to 25 August 1978.
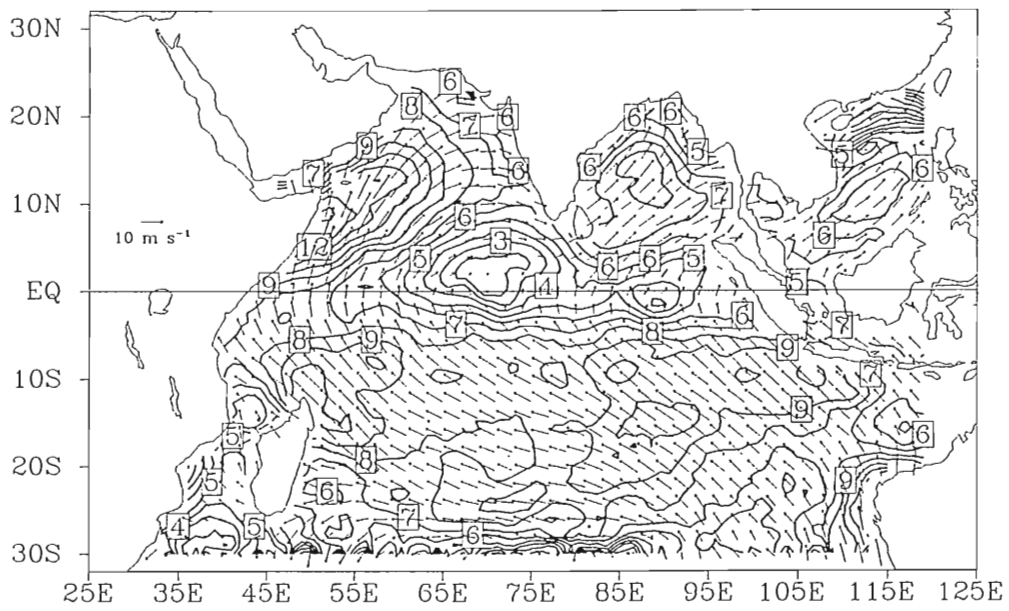
Figure 24.   Resultant field for the period 26 August to 30 August 1978.
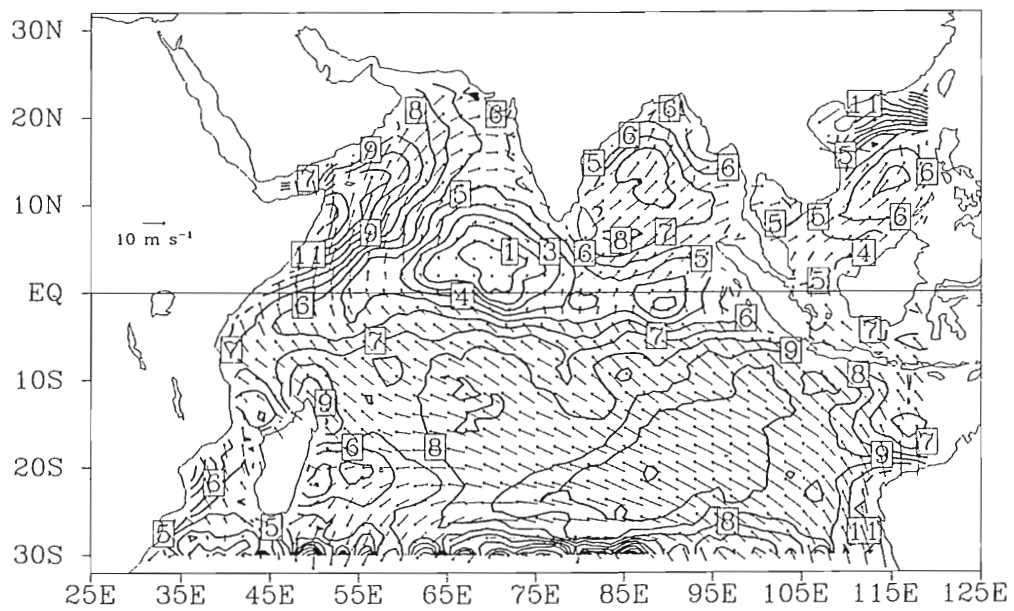
Figure 25.   Resultant field for the period 31 August to 4 September 1978.
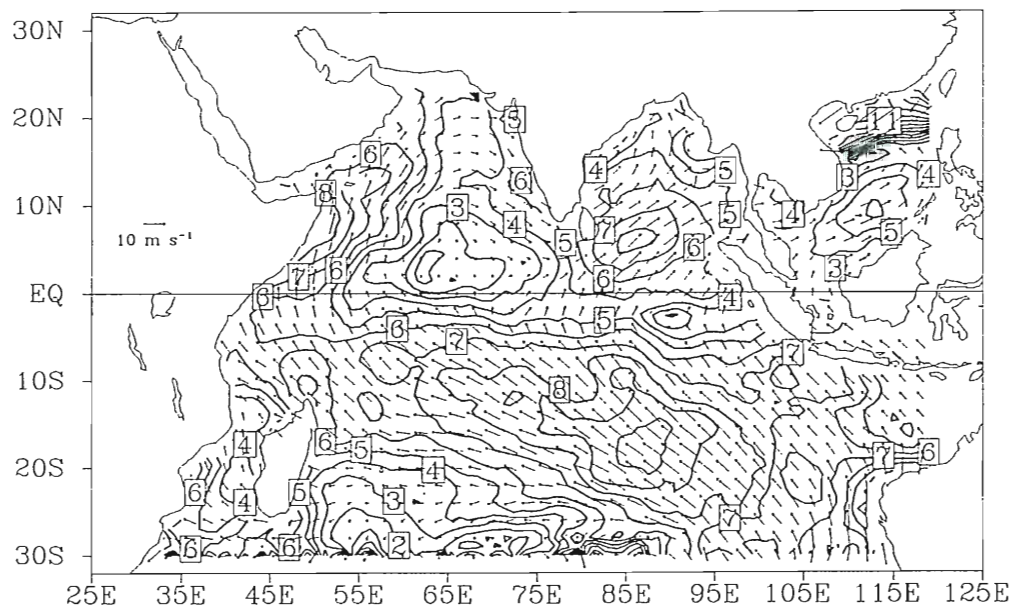
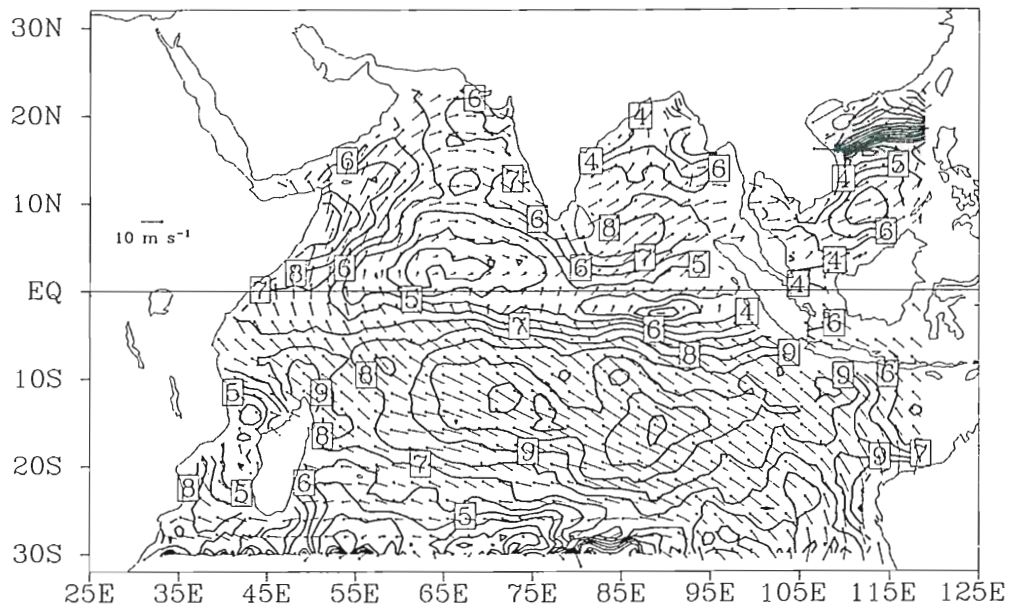Figure 26.   Resultant field for the period 5 September to 9 September 1978.

Figure 27.   Resultant field for the period 10 September to 14 September
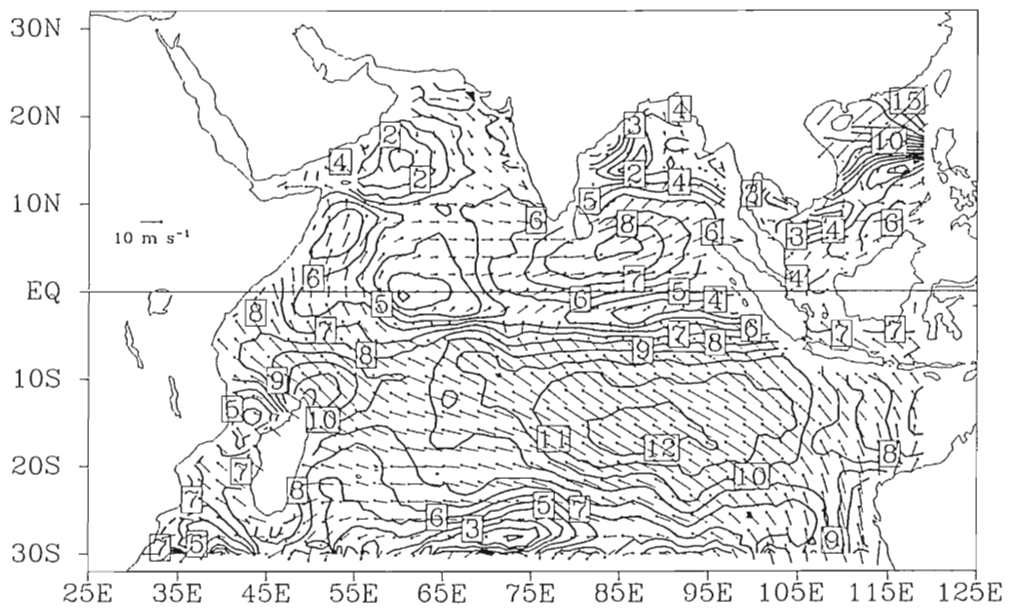1978.

Figure 28.   Resultant field for the period 15 September to 19 September
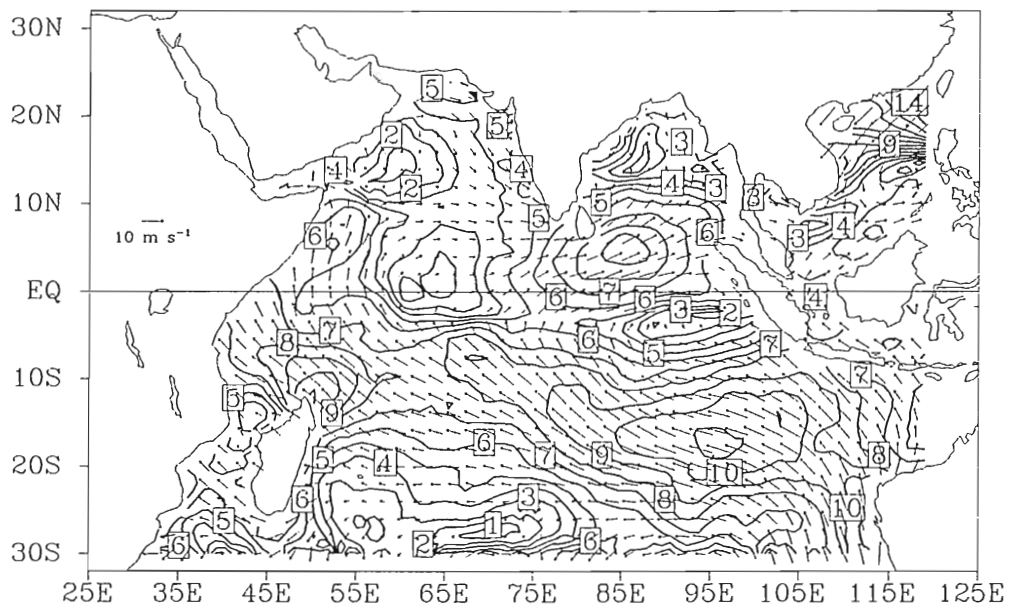1978.

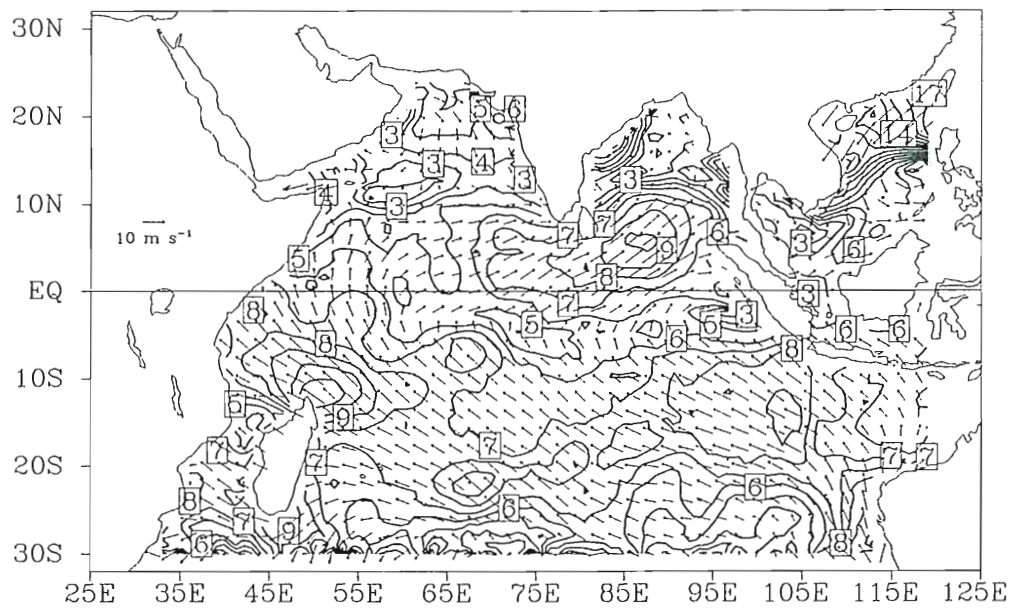Figure 29.   Resultant field for the period 20 September to 24 September 1978.

Figure 30.   Resultant field for the period 25 September to 29 September
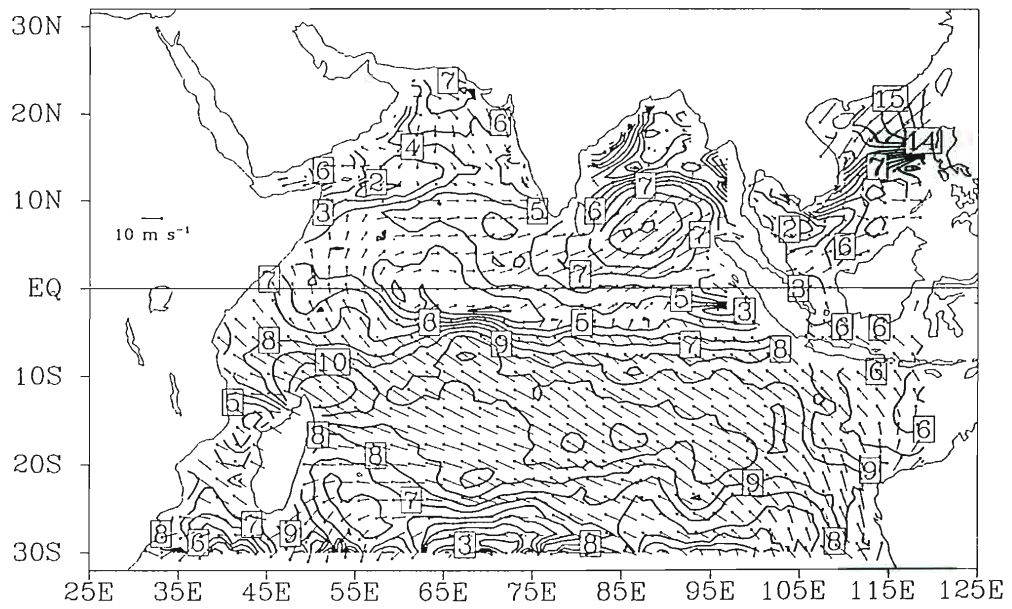   1978.

Figure 31.   Resultant field for the period 30 Spetember to 4 October 1978.

References

Bruce, J.G., 1983: The wind field in the Western Indian Ocean and the related ocean circulation. *Mon.. Wea.. Rev.* , **111**, 1442-1452.

Cacuci, D.G., 1988: The forward and adjoint method of sensitvity analysis, In: Ronan, Y., ed., *Uncertainty Analysis* , CRC Press, 282 pp.

Estoque, M.R. and J.J. Fernandez-Partagas, 1980: Analysis of Seasat wind observations over the Indian Ocean. University of Miami Technical Report Number TR - 80 - 3, 55 pp.

Gill, P.E., W. Murray, M. Wright, 1981: *Practical Optimization*. Academic Press, 401 pp.

Harlan, J., Jr. and J.J. O'Brien, 1986: Assimilation of scatterometer winds into surface pressure fields using a variational method. *Jou. Geophys. Rea.* , **91**, 7816-7836.

Hastenrath, S., and P. Lamb, 1979: *Climatic Atlas of the Indian Ocean Part I: Surface Climate and Atmospheric Circulation*. Univ. of Wisconsin Press, 97 pp.

Hastenrath, S., 1991: *Climate Dynamics of the Tropics*, Kluwer Academic Publishers, 488 pp.

Hoffman, R., 1982: SASS wind ambiquity removal by direct minimization. *Mon. Wea. Rev.* , **110**, 434-445.

Hoffman,R., 1984: SASS wind ambiquity removal by direct minimization. Part II: Use of smoothness and dynamical constraints. *Mon. Wea. Rev.*, **112**, 1829-1852.

Part II: Use of smoothness and dynamical constraints. *Mon. Wea. Rev.*, **112**, 1829-1852.

Kalnay, E., and R. Atlas, 1986: Global analysis of ocean surface wind and wind stress using a general circulation model and Seasat scatterometer winds. *Jou. Geophys. Res.*, **91**, 2233-2240.

Legler, D.M., I.M. Navon, and J.J. O'Brien, 1989: Objective analysis of pseudostress over the Indian Ocean using a direct-minimization approach. *Mon. Wea. Rev.*, **117**, 709-720.

Legler, D.M., 1991a: Producing surface wind products for oceanographers. *Papers presented at the joint IOC/WMO seminar on IGOSS products*, 59-76.

Legler, D.M., 1991b: Errors of five-day mean surface wind and temperature conditions due to inadequate sampling. *Jou. Atm. and Ocean Technology*, **8**, 705-712.

Legler, D.M., 1992: Analysis of air and sea physical properties and surface fluxes using a combination of in-situ and SEASAT data. *Ph D Dissertation*, Florida State University, 135 pp.

Meyers, S.D., C.S. Jones, D.M. Legler, K.F. Miles, and J.J. O'Brien, 1992: The sensitivity of direct minimization technques to parametric variations. work in progress.

Navon, I.M., D. M. Legler, 1987: Conjugate-gradient methods for large-scale minimization in meteorology. *Mon. Wea. Rev.*, **115**, 1479-1502.

O'Brien, J., R. Kirk, L. McGoldrick, J. White, R. Atlas, E. Bracalente, O. Brown, R. Haney, D.E. Harrison, D. Honhart, H. Hurlburt, R. Johnson, L. Jones, K. Katsaros, R. Lambertson, S. Peteherych, W. Pierson. J. Price, D. Ross, R. Stewart, and P. Woiceshyn, 1982: Scientific opportunities using satellite surface wind stress measurements over the ocean. *Report of the Satellite Surface Stress Working Group*, Nova University/ N.Y.I.T. Press, Fort Lauderdate, FL, 153 pp.

Pierson, W., Jr., 1990: Examples of, reasons for, and consequences of the poor quality of wind data from ships for marine boundary layer: implications for remote sensing. *Jou. Geophys. Rea.*, **95**, C8, 13313-13340.

Rao, G.V., H.M.E. van de Boogaard, and W.C. Bolhofer, 1978: Further 13340.

Rao, G.V., H.M.E. van de Boogaard, and W.C. Bolhofer, 1978: Further calculations of sea level air trajectories over the equatorial Indian Ocean. *Mon. Wea. Rev.*, **106**, 1465-1475.

Rao, G.V., W.R. Schaub,Jr, and J. Puetz, 1981: Evaporation and Precipitation over the Arabian Sea During Several Monsoon Seasons. *Mon. Wea. Rev.* , **109**, 364-370.

Sasaki, Y., 1958: An objective analysis based on the variational method. *Jou. Met. Soc. Japan*, **36**, 77-88.

Shanno, D.F., and K.H. Phua, 1980: Remark on algorithm 500 - a variable method subroutine for unconstrained nonlinear minimization. *ACM Trans. Math. Softw.* , **6**, 618-622.

Slutz, R.J., S.J. Lubker, J.D. Hiscox, S.D. Woodruff, R.L. Jenne, D.H. Joseph, P.M. Steurer, and J.D. Elms, 1985: *COADS Comprehensive Ocean-Atmosphere Data Set Release 1*. CIRES University of Colorado. 300 pp.

Stephens, J.J., 1965: A variational approach to numeriacal weather analysis and prediction, *PhD Dissertation*, The University of Texas, 243 pp.

Stout J.E., and J.A. Young, 1983: Low-level monsoon dynamics derived from Satellite Winds. *Mon. Wea. Rev.* , **111**, 774-798.

Yasunari, T., 1991: The monsoon year - a new concept of the climatic year in the tropics. *Bull. Amer. Meteor. Soc.*, **72**, 1331-1338.

Biographical Sketch

Kelley Franklin Miles was born in Thomaston, Georgia in 1968 and grew up there. After attending the Georgia Institiute of Technology for one year, he began the program in meteorology at the Florida State University. He received his Bachelor's Degree in Meteorology in June, 1990 and began graduate school at Florida State in August, 1990. He began research with Dr. James O'Brien in January, 1991 upon obtaining an Office of Naval Research Grant. He obtained a Master's Degree in Physical Meteorology in December, 1992.